IRD
Institut de recherche
pour le développement

Field tests of NUMIS^{plus} MRS equipment in northern Denmark (August 2003)

September 2003

IRD report

Field tests of NUMIS^{plus} MRS equipment in Denmark

Institut de Recherche pour le Développement

32, avenue Henri Varagnat, 93143, Bondy cedex, France

Field tests of NUMIS^{plus} MRS equipment in northern Denmark (August 2003)

Anatoly Legchenko and Henri Robain

September 2003

IRD report

Key words: geophysics, groundwater, magnetic resonance sounding, nuclear magnetic resonance, MRS, NMR, SNMR.

In bibliography, this report should be cited as follows:

Anatoly Legchenko and Henri Robain, (2003) – Field tests of NUMIS^{plus} MRS equipment in northern Denmark (August 2003). IRD report, 71 p., 28 fig., 3 tabl., 1 ann.

Abstract

Magnetic Resonance Sounding (MRS) is distinguished from other geophysical tools used for ground water investigation by the fact that it measures a magnetic resonance signal generated directly from subsurface water molecules. An alternating current pulse energizes a wire loop on the ground surface and the MRS signal is generated; subsurface water is indicated, with a high degree of reliability, by non-zero amplitude readings. Measurements with varied pulse magnitudes then reveal the depth and thickness of water-saturated layers. The hydraulic conductivity of aquifers can also be estimated using boreholes for calibration. MRS can be used for both predicting the yield of water supply wells, and for interpolation between boreholes, thereby reducing the number of holes required for hydrogeological modeling.

With a goal of testing the efficiency of this technique in Denmark, field tests were carried out in cooperation with Aahrus University (Denmark) by the Institut de Recherche pour le Développement (IRD, France) in northern Denmark between 20 and 29 August 2003. During the fieldwork the NUMIS^{plus} MRS instrument produced by IRIS Instruments (France) was used.

In this report, the basic principles of the method and the results of the field tests are presented.

Table of contents

List of figures

List of tables

Introduction

Magnetic Resonance Sounding (MRS) is sensitive specifically to ground water because subsurface water molecules generate a magnetic resonance signal that can be recorded. This direct detection of subsurface water is the main advantage of MRS compared with other geophysical tools used for hydrogeological investigation.

MRS is a large-scale method, and the investigated volume can be approximated by a cube of $1.5 \times a$ where $10 \le a \le 150$ m is the side of a square loop. The method, with 'HYDROSCOPE' equipment, was developed in Russia during the early nineteen eighties (Semenov et al. 1989) and proved the possibility of non-invasive detection of aquifers using magnetic resonance measurements. At that time, only the geometry and water content of water-saturated layers could be obtained using MRS. Further developments, and experience of MRS practical applications, made possible the estimation of aquifer hydraulic conductivity, for which the water content w and relaxation time T_1 were derived from MRS measurements and used with an empirical relationship borrowed from Nuclear Magnetic Resonance Logging (NML). In practice however, it is often more reliable to use MRS estimates of transmissivity than hydraulic conductivity, and there is generally good correlation between MRS transmissivity estimates and those indicated by borehole pumping tests.

In August 2003, a field survey was carried out in northern Denmark by the Institut de Recherche pour le Développement (IRD, France) in cooperation with Aahrus University (Denmark). The goal of this work was to test the efficiency of a combined geophysical approach (TEM+MRS) applied to localization of glacial deposits that are potential aquifers in Denmark and characterization of their hydrodynamic properties. For the fieldwork, NUMIS^{plus} MRS instrument produced by IRIS Instruments (France) and GEONICS (Canada) Transient EM system PROTEM were used.

In this report, the basic principles of the MRS method and the results of the field tests are presented.

1. Magnetic Resonance Sounding method

1.1. BASIC PRINCIPLES

To an outside observer, the MRS field set-up appears very similar to that of Transient EM with a coincident transmitting/receiving loop. A wire loop is laid out on the ground, normally in a circle of 10 m to 150 m diameter depending on the depth of the target aquifer. The loop may also be laid out in a square or, to improve signal to noise ratio (S/N), in a "figure of eight" shape (Trushkin et al. 1994).

The method is based on fact that protons possess a non-zero magnetic moment. The resonance behaviour of proton magnetic moments in the geomagnetic field ensures that the method is selective and sensitive only to ground water. The resonance frequency $\omega_0 = 2\pi f_0$ is given by the spin Larmor resonance condition $\omega_0 = \gamma_p B_0$, with B_0 being the magnitude of the geomagnetic field and $\gamma_p / 2\pi = 4.257707 \times 10^7$ Hz/T the gyromagnetic ratio for protons. The Larmor frequency is obtained from measurements of the geomagnetic field (B_0) on the surface using a proton magnetometer. Depending on the global geographical location of the investigated area, the geomagnetic field varies between approximately 20,000 and 60,000 nT, and the Larmor frequency correspondingly varies between 800 and 2800 Hz.

Using the classical model (Slichter 1990), in which the coordinate system rotates with an angular frequency $\omega = -\gamma B_0$, the local macroscopic spin magnetization of protons in a water sample dV can be presented as vector $\mathbf{M}$ with the amplitude $M = |\mathbf{M}| = M_0 dV$, where $M_0 = 3.287 \times 10^{-3} B_0$ at 293°K (20°C) and is the spin

magnetization of hydrogen protons per unit volume. In the equilibrium position, **M** is oriented along the geomagnetic field and the angle θ between the spin magnetization and the geomagnetic field is equal to zero ($\theta = 0$) as it is shown in Figure 1a.

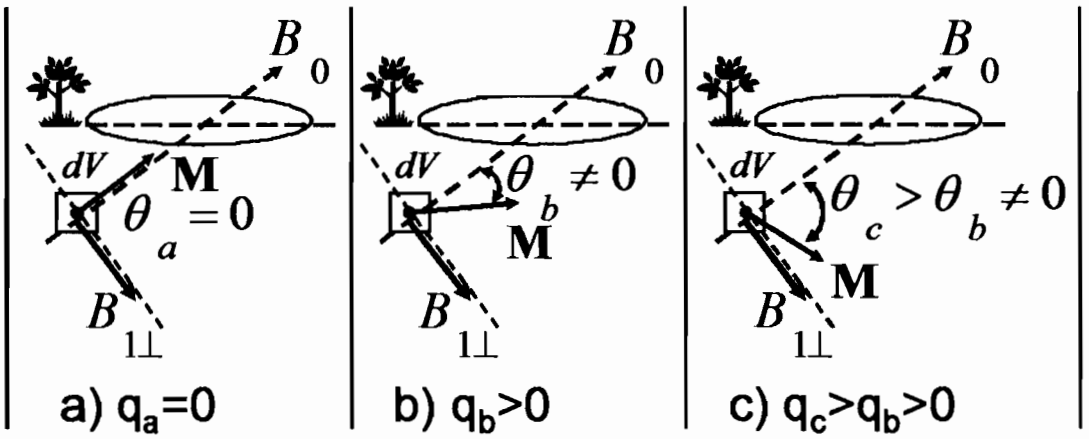

Figure 1. Precession of spin magnetization in rotating with the Larmor frequency coordinate system.

The magnetic resonance signal is generated only by a perpendicular to the earth's magnetic field component of the spin magnetization $M_{\perp} = M\sin(\theta)$, so no signal exists at this time. A pulse of alternating current then energizes the MRS loop:

$$i(t) = I_0 \cos(\omega_0 t), \quad 0 < t \le \tau, \qquad (1)$$

where I_0 and τ are respectively the pulse amplitude and duration. The pulse causes precession of the spin magnetization around the geomagnetic field, which produces a non-zero flip angle (Figure 1b):

$$\theta = \frac{\gamma_p B_{1\perp}(\mathbf{r})}{2I_0} q, \qquad (2)$$

where $q = I_0 \tau$ is the pulse parameter, $B_{1\perp}(\mathbf{r})$ is a perpendicular to the geomagnetic field component of the loop magnetic field, and $\mathbf{r} = r(x, y, z)$ is the coordinate vector. For a sample $dV(\mathbf{r})$, the flip angle θ is larger for larger values of the pulse parameter q (Figures 1b and 1c). Transmissions from the loop magnetic field can be calculated accurately (Weichman et al. 2000), but in general they decrease with increased distance r between the loop and the sample $dV(\mathbf{r})$ as a cubic function ($B_{1\perp}/I_0 \sim 1/r^3$). Consequently, for fixed q, the flip angle θ depends on the water location. The magnetic resonance signal is proportional to θ ($M_\perp = M\sin(\theta)$) and thus, by measuring the signal on the surface for various values of the pulse parameter q, the location of a water sample $dV(\mathbf{r})$ can be derived from Equation 2. This is the principle of Magnetic Resonance Sounding.

Water content

Precession of the spin magnetization $\mathbf{M}$ around the geomagnetic field caused by the current pulse in the loop creates an alternating magnetic field that can be measured, using the same loop, after the pulse cut-off. Oscillating with the Larmor frequency, the magnetic resonance signal $e(t)$ has an exponential envelope and is a function of the pulse parameter q:

$$e(t,q) = e_0(q)\exp\left(-t/T_2^*(q)\right)\sin\left(\omega_0 t + \varphi_0(q)\right), \qquad (3)$$

where $T_2^*(q)$ is the spin-spin relaxation time, and $\varphi_0(q)$ is the phase.

The signal induced in the receiver loop is proportional to the sum of the flux of all precessing magnetic moments $M_\perp$. Using the reciprocity theorem, and neglecting the higher harmonics of the pulse and a possible frequency offset between the Larmor frequency and the current frequency, the induction in the loop voltage thus becomes (Legchenko et al. 2002a)

$$e_0(q) = \frac{M_0 \omega_0}{I_0} \int_V B_{1\perp}(\mathbf{r}) e^{j2\varphi_0(\mathbf{r})} \sin(\theta(\mathbf{r},q)) w(\mathbf{r}) dV(\mathbf{r}), \qquad (4)$$

where φ_0 is the phase shift caused by electrically conductive rocks, and $0 \le w(\mathbf{r}) \le 1$ is the water content. As both $M_0 = \gamma_p B_0$ and $\omega_0 = \gamma_p B_0$ are proportional to the geomagnetic field, it follows from Equation 4 that the amplitude of the magnetic resonance signal depends on the geographical location of the investigated area $e_0 \sim B_0^2$ (Legchenko et al. 1997).

Assuming that the stratification is horizontal, and the vertical distribution of resistivity is known, Equation 4 of the signal amplitude e_0 can be simplified to a Fredholm linear integral equation of the first kind (Legchenko and Shushakov 1998):

$$e_0(q) = \int_0^L K(q,z) w(z) dz, \qquad (5)$$

where $K(q,z) = \frac{M_0 \omega_0}{I_0} \int_{x,y} B_{1\perp}(\mathbf{r}) \sin(\theta(\mathbf{r},q)) dx dy$.

Numerical results show that distant protons produce a negligibly small signal and, hence, integration can be limited by approximately $x^2 + y^2 < (1.5D)^2$, where D is the loop diameter (or side for a square loop). Consequently, $L = 1.5D$ can be considered as the maximum possible depth of water detection by MRS, and a cube with side $1.5D$ as the approximate maximum possible volume. It should be noted that in heterogeneous geological environments, MRS data about aquifers are the averages of readings for a volume proportional to the size of the loop.

The vertical distribution of water content $w(z)$ is resolved by Equation 5. This linear equation may be solved by projecting it onto finite dimensional subspace, as approximated by the projected equation

$$\sum_j \left(h_j(q_i) w_j \right) = e_{0i}, \qquad (6)$$

where $i = 1,2,..,I$, $j = 1,2,..,J$ and $h_j(q)$ is a set of kernel vectors obtained by projecting the kernel $K(q,z)$ on a set of basis functions $b_j(z)$, so that

$$w(z) = \sum_j \left(w_j b_j(z) \right), \qquad (7)$$

and $h_j(q) = \int_0^L K(q,z) b_j(z) dz$.

From a physical point of view, the problem allows the basis functions to be assumed as box-car functions. Hence, the kernel vectors are the elementary responses from the layers of water ($w_j = 1$), characterized by their depth z and thickness Δz. If the depth intervals are $0 \le z \le L$, $\Delta z_j = z_{j+1} - z_j$ and $L = \sum_{j=1}^{J} \Delta z_j$ then the basis functions are $b_j(z_j \le z < z_{j+1}) = 1$, $b_j(z < z_j, \quad z \ge z_{j+1}) = 0$ and the kernel vectors are

$$h_j(q) = \int_{z_j}^{z_{j+1}} K(q,z) dz. \qquad (8)$$

In a matrix notation, projected Equation 6 can be written as

$$\mathbf{A}\mathbf{w} = \mathbf{e}_0, \qquad (9)$$

where $\mathbf{A} = \left[a_{i,j} \right]$ is a rectangular matrix of $I \times J$ with the elements $a_{i,j} = h_j(q_i)$, $\mathbf{e_0} = (e_{01}, e_{02}, ..., e_{0i}, ..., e_{0I})^T$, $e_{0i} = e_0(q_i)$ being the set of experimental data, $\mathbf{w} = (w_1, w_2, ..., w_j, ..., w_J)^T$, $w_j = w(\Delta z_j)$ being the vertical distribution of water content, and the symbol T denoting transposition. The inversion was carried out according to the well-known Tikhonov regularization method (Tikhonov and Arsenin 1977).

The MRS inverse problem is ill-posed. It means that it is impossible, for a particular layer, to know both the layer thickness and the water content, what is giving rise to layer equivalence. Two layers at the depth z_e with the thicknesses $\Delta z_1, \Delta z_2 < \Delta z_e$ are equivalent if $w_1 \Delta z_1 = w_2 \Delta z_2$. The equivalent layers cannot be resolved. The thickness Δz_e is defined by the vertical resolution of the method which depends on the magnetic field created by the loop; the larger the gradient of the field, the better the resolution. The magnetic field of a loop on the surface with a current passing through is well known; the gradient of the field is large close to the surface and decreases with increasing depth. Consequently, the resolution of the MRS is also better close to the surface. Figure 2 shows the relative errors of resolution for a synthetic model consisting of a 10-m-thick layer ($w = 20\%$) versus the layer depth. A square 100-m-side loop is assumed.

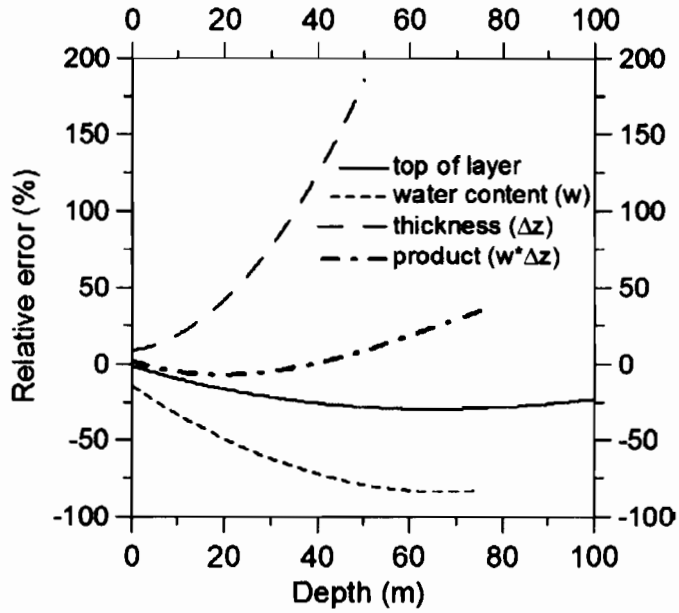

Figure 2. Numerical modeling: resolution of a 10 m-thick layer when using 100 m-side square loop.

The errors were calculated as $\varepsilon = 100\% \times (P_{inv} - P_{\mathrm{mod}}) / P_{\mathrm{mod}}$, where P_{inv} and P_{mod} are, respectively, a parameter from the inversion and its true value given by the model. It can be seen that both the water content and the thickness are better resolved when the layer is close to the loop, and that errors increase with distance from the loop. At a depth greater than about one half of the loop side, the 10-m-thick layer cannot be resolved. However, note that the resolution accuracy of the product $w \times \Delta z$ is much better.

In practice, measurement of the signal is not possible without an instrumental delay ("dead time") of τ_d. Consequently, for each value of q, the initial amplitude e_0 cannot be measured but is obtained by the extrapolation

$$e_0 = e(\tau_d) \exp(\tau_d / T_2^*). \qquad (10)$$

The non-linear fitting scheme of Legchenko and Valla (1998) is used for estimating $e(\tau_d)$ and T_2^* from records after the pulse time series. The pulse duration for currently available MRS instruments is about 40 ms and the "dead time" is $\tau_d = 30 \div 40$ ms; this is a limitation that does not allow measuring short signals with $T_2^* < 30$ ms.

The water content derived from MRS data is calculated as follows:

Let V be the total volume of the subsurface; V_W and V_A, the parts of subsurface filled with water and air respectively, and V_R the part of subsurface occupied by rocks. Thus, $V = V_W + V_A + V_R$. The water (V_W) can be separated into two parts: water V_{short}, characterized by a very short MRS signal which cannot be measured by MRS instruments, and water V_{long} that produces a measurable signal with sufficiently long relaxation time ($V_W = V_{short} + V_{long}$). Thus, the MRS water content can be defined as the part of the total volume of the subsurface occupied by measurable MRS water: $w = \frac{V_{long}}{V} 100\%$.

Water in porous media can be divided into two parts (after Castany 1982): capillary-bound water and free water ($V_W = V_{bound} + V_{free}$). The capillary-bound water (V_{bound}) is attached to grain walls and cannot be extracted by gravity. The free water (V_{free}) is located some distance from the grain walls and, therefore, can be extracted by gravity. Capillary-bound water generally dominates in the unsaturated zone, but both capillary-bound and free water are normally present in the aquifer. In highly permeable water-saturated rocks such as sand or gravel, most of the water is free. On the contrary, in water-saturated rocks with low permeability, such as clay, most of the water is capillary-bound. Experiences of magnetic resonance measurements in porous media

show that capillary-bound water is characterized by shorter relaxation times, and free water by longer relaxation times (Chang et al. 1997). In some rocks, capillary-bound water may have $T_2^* < 30$ ms, and free water $T_2^* > 30$ ms. As MRS instruments are able to measure only relatively long signals ($T_2^* > 30$ ms), it is clear that in these rocks MRS is sensitive mostly to free water (Schirov et al. 1991).

In nuclear magnetic resonance logging, the magnetic resonance response is correlated with the effective porosity. Obviously, MRS water content w is also related to the effective porosity, but there is currently insufficient experimental data to establish a quantitative relationship.

The relationship between measured signal $e_0(q)$ and water content $w(z)$ shown in Equation 5 was verified experimentally in the early 1980s, when field measurements were carried out on an ice (0.8 m thick) covered lake in Russia using HYDROSCOPE equipment (Schirov et al. 1991). The magnetic resonance signal from bulk water in the lake has a long relaxation time ($T_2^* > 800$ ms) and, hence, all the water contributes to the MRS water content. The theoretical signal calculated for the model of a 10-m-thick water body ($w = 100\%$), derived from mapping the lake bottom, fits particularly well with the initial part of the experimental data where the contribution of lake water into the total signal is maximal (Figure 3). No information was available about possible aquifers below the lake, so MRS data for greater depths could not be evaluated.

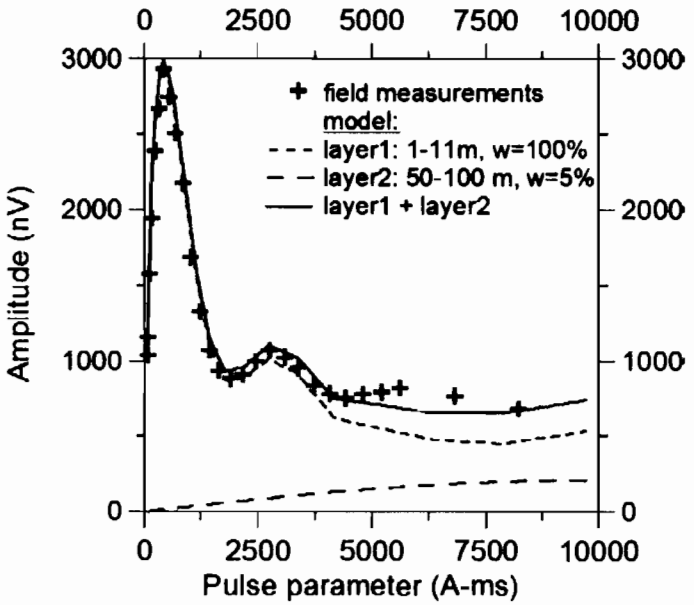

Figure 3. Frozen lake experiments (Schirov et al. 1991): comparison of measured and theoretical signals.

Relaxation Times

Other important characteristics of the magnetic resonance signal are; longitudinal relaxation time T_1, transverse relaxation time T_2, and the observed relaxation time T_2^* (Slichter 1990). In porous media, the relaxation times T_1 and T_2 ($T_1 \approx 1.5 \times T_2$) are proportional to the mean pore size (Kleinberg et al. 1994; Kenyon 1997):

$$T_{1(2)} \approx \frac{V_p}{\rho_{1(2)} S_p}, \qquad (11)$$

where S_p and V_p are the surface and volume of pores respectively; and $\rho_{1(2)}$ is the surface relaxivity (when using T_1 or T_2), which depends on rock mineralogy. In

magnetic resonance logging, both T_1 and T_2 are used for estimating aquifer permeability.

Because of technical difficulties with measuring T_1 and T_2 in large volumes from the surface, only the MRS T_2^* relaxation time, which can be derived from the envelope of the magnetic resonance signal (Equation 3), was used initially (Schirov et al. 1991). Whilst it is known that T_2^* is proportional to T_2, T_2^* is also sensitive to local inhomogeneities in the geomagnetic field ΔB_0 caused by rocks (Farrar and Becker 1971);

$$\frac{1}{T_2^*} = \frac{1}{T_2} + \gamma_p (\Delta B_0 / 2), \qquad (12)$$

which makes T_2^* less reliable than T_1 or T_2 for pore size estimation.

Examples of T_2^* and T_1 measurements in rocks with different magnetic properties are presented in Table 1 (Legchenko et al. 2002b).

Rock type	Magnetization (A/m)	Susceptibility (SIU)	T_2^* (ms)	T_1 (ms)	Comments
Reef limestone (Cyprus)	1×10^{-4}	-9.1×10^{-6}	80	220	Unsaturated zone
Fractured limestone (Cyprus)	2.8×10^{-4}	-8.5×10^{-6}	130	430	Aquifer
Highly fractured limestone (France)	8.1×10^{-3}	1.5×10^{-3}	280	800	Aquifer
Karst limestone (Cyprus)	4.5×10^{-5}	-7.2×10^{-6}	460	1000	Aquifer
Clay and fine sand (France)	1.4×10^{-3}	1.4×10^{-4}	70	310	Aquifer
Medium sand (France)	3.9×10^{-4}	2.9×10^{-5}	120	420	Aquifer
Gravel and coarse sand (France)	7.5×10^{-4}	4.4×10^{-4}	330	600	Aquifer
Sandstone (USA)	3.2×10^{-4}	2×10^{-4}	80	-	Aquifer
Basaltic gravel (Cyprus)	1.3×10^{-1}	4.8×10^{-3}	10	-	Aquifer

Table 1. Magnetic properties of rocks and MRS relaxation times.

The magnetization and magnetic susceptibilities of the rocks were measured in the laboratory with rock samples prepared either as 8 cm^3 solid cubes or 5.4 cm^3 powder volumes, depending on the rock material. Measurements were carried out using a JR5 instrument (AGICO, Geofysika) with a sensitivity of 2.4×10^{-6} A/m, and a KLY-3S instrument (AGICO, Geofysika) with a sensitivity of 3×10^{-8} SIU. Relaxation times were measured from the surface with a NUMIS MRS instrument that covered large volumes. In limestone, the signals from both free and capillary-bound water were relatively long ($T_2^* > 70 \div 80$ ms), considering the threshold of the MRS instruments (30 ms). On the contrary, in basaltic gravel even the signal from free water was very short ($T_2^* \approx 10$ ms) and, therefore, cannot be measured with a standard MRS instrument.

For this reason, measurements in the basaltic gravel were carried out using a NUMIS non-standard setup, which was adapted to the spin echo technique (Farrar and Becker 1971) especially for these experiments.

Thus, in non-magnetic rocks like limestone, both free and capillary-bound water contribute to MRS water content. In magnetic rocks however, even free water cannot be detected. It should be also added that other factors, such as surface relaxivity, and the temperature and salinity of water, may influence MRS measurements (Dunn et al. 2002). This suggests the possibility of correlating MRS responses with different geological formations.

The saturation recovery method (Dunn et al., 2002) can be used for measuring T_1. This consists of applying two pulses, separated by a delay τ_p, to the investigated sample and measuring the magnetic resonance response after the second pulse. Each pulse flips the spin magnetization to the exact angle of $\pi/2$. Under laboratory conditions, only small samples are investigated and special care is taken to have both the static and alternating magnetic fields as homogeneous as possible inside the sample. In the laboratory, therefore, the pulses can be set up so that the flip angle is equal to exactly $\pi/2$. In field conditions however, the flip angle in a volume dV depends on its distance from the surface loop and, within the studied volume, the flip angle caused by the same pulse may vary widely for different samples $dV(\mathbf{r})$, which is why T_1 cannot be measured directly.

The saturation recovery method, however, can be adapted to MRS. Two pulses are applied to the investigated volume and, after the first pulse, the spin magnetization $\mathbf{M}$ of the sample dV is turned off at the angle θ (Equation 2), as shown in Figure 1. During the delay τ_p, it builds up towards equilibrium along the geomagnetic field with the time constant T_1. Assuming the spin system to be linear, and neglecting relaxation during the pulse, ($\tau << T_2^*, T_2, T_1$), the perpendicular to the earth's magnetic field

component of the spin magnetization after the second pulse can be described by the equation:

$$M_{\perp}(\tau_p) = M_0 \exp(-\tau_p / T_1)\sin(\theta + \theta_2) + M_0\left(1 - \exp(-\tau_p / T_1)\right)\sin(\theta_2), \quad (13)$$

where θ_2 is the flip angle caused by the second pulse. If both pulses are set to be equal ($q_1 = q_2 = q$) and the phase shift between the current of the second pulse is equal to 180° relative to the current of the first pulse, then $\theta_2 = -\theta$ and Equation 13 can be simplified to:

$$M_{\perp}(\tau_p) = -M_0\left(1 - \exp(-\tau_p / T_1)\right)\sin(\theta). \quad (14)$$

For calculating the amplitude of a MRS signal measured after the second pulse, Equation 4, which describes the amplitude after the first pulse will be replaced by:

$$e_{02}(q, \tau_p) = \frac{M_0 \omega_0}{I_0} \times \quad . \quad (15)$$

$$\times \int_V \left(1 - \exp\left(-\tau_p / T_1(\mathbf{r})\right)\right) B_{1\perp}(\mathbf{r}) e^{j(2\varphi_0(\mathbf{r}) + \pi)} \sin\left(\theta(\mathbf{r}, q)\right) w(\mathbf{r}) dV(\mathbf{r})$$

If horizontal stratification is assumed and:

$$x(z) = 1 - \exp\left(-\tau_p / T_1(z)\right), \quad (16)$$

then Equation 15 can be resolved by applying the same approach as for the resolution of Equation 4. Thus, using the notations introduced for Equation 9, and just one value for the delay between the pulses fixed at $\tau_p = (2 \div 3) \times T_2^*$, it follows that:

$$(\mathbf{Aw})\mathbf{x} = \mathbf{e}_{02}, \quad (17)$$

where the water content $\mathbf{w}$ is obtained by the resolution of Equation 9, $\mathbf{e}_{02}$ is the set of experimental data measured after the second pulse, and $\mathbf{x} = (x_1, x_2, ..., x_j, ..., x_J)^T$ is the solution vector. Equation 16 allows easy calculation of $T_{1J} = -\tau_p / \log(1 - x_j) = T_1(\Delta z_j)$, which is a vertical distribution of the relaxation time T_1. If it is possible to carry out measurements with different values of τ_p, then this will improve the accuracy of results, but will also increase time required for the data acquisition.

It is instructive to now compare T_1 measurements at two different sites. The Site 1 aquifer is composed of coarse sand, and the borehole yield is about 120 m^3/h. The Site 2 aquifer is composed of chalk, and the borehole yield is about 3 m^3/h. For demonstration purposes, T_1 was measured for just one value of the pulse parameter q, with varied delays between the pulses τ_p, which gives the apparent relaxation time $T_{1a}(q)$ rather than real one $T_1(z)$. However, as only one aquifer exists at each of these sites, the apparent T_{1a} may be considered as the real T_1. Normalized amplitudes measured at each site versus the delay τ_p are shown in Figure 4. As expected, a longer T_1 was observed at the site where the aquifer has a larger yield.

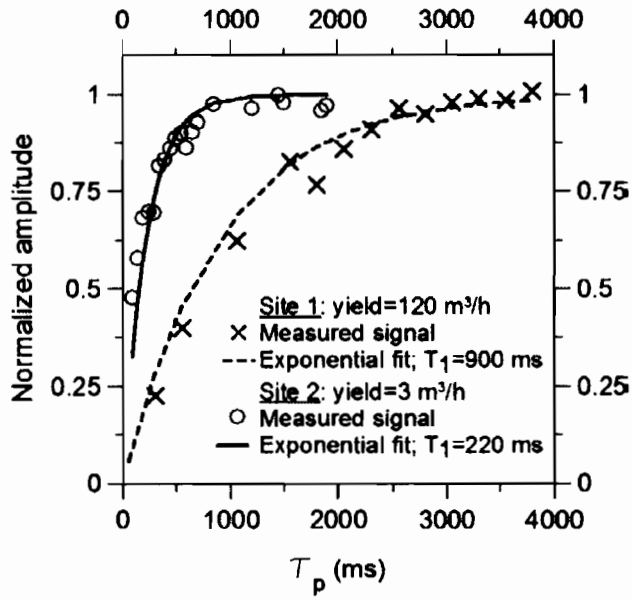

Figure 4. Comparison of two different aquifers: normalized amplitude of the MRS signal measured after the second pulse versus the delay between the pulses.

MRS estimation of hydraulic conductivity

In nuclear magnetic resonance logging, the permeability of water-saturated porous media can be estimated as (Chang et al. 1997; Kenyon 1997):

$$k_{NML} = a\phi_{NML}^{b} T_1^{c}, \qquad (18)$$

with k_{NML} being the permeability estimated using magnetic resonance data, ϕ_{NML} and T_1 the porosity and the relaxation time derived from NML measurements, and a, b, c are empirical constants. Other formula, such as $k_{NML} = aT_2^{b}/F^{c}$, where a, b, c are empirical constants and F is the electrical formation factor, have been also suggested (Wyllie and Spangler 1952). Both formula work equally well within experimental errors. Different estimation methods, based on Equation 18, have also been developed; first, $b = 1$ and $c = 2$ were proposed by Seevers (1966), and later it

was shown that, for sandstones, better accuracy can be achieved using $b = 4$ and $c = 2$ (Timur 1968, 1969a, 1969b; Kenyon et al. 1988). In MRS, a formula based on Equation 18 is actually used for estimating the hydraulic conductivity

$$K_{MRS} = C_p w^a T_1^b. \qquad (19)$$

Hydraulic conductivity is a scale-dependent parameter. Taking into account that MRS results are averaged over a large area defined by the loop size, the pumping tests, which also provide results averaged over a large volume, are used for calibration.

Pumping test transmissivity values reflect the hydraulic conductivity and thickness of the aquifer $T_{bh} = K_{bh} \Delta z_{bh}$. Estimates of both hydraulic conductivity and aquifer thickness can be derived also from MRS measurements, and the MRS transmissivity estimate is:

$$T_{MRS} = \int_{\Delta z} K_{MRS}(z) dz, \qquad (20)$$

where $K_{MRS}(z) = C_p w^a(z) T_1^b(z)$, and Δz is the thickness of the aquifer estimated by MRS.

Two estimators, based on Equation 19 ($\sim wT_1^2$ and $\sim w^4 T_1^2$), were tested using MRS measurements in France (an area between Chartres and Orleans). For each estimator, the constant C_p was selected so that the MRS estimated transmissivities matched the best pumping test transmissivities. It was found that, when applied to MRS measurements, the ($\sim wT_1^2$) estimator gave better results than the reportedly more accurate ($\sim w^4 T_1^2$) estimator. A comparison between the MRS and borehole pumping test results is shown in Figure 5; the error bars were calculated taking into account the accuracy of MRS data and possible equivalent solutions.

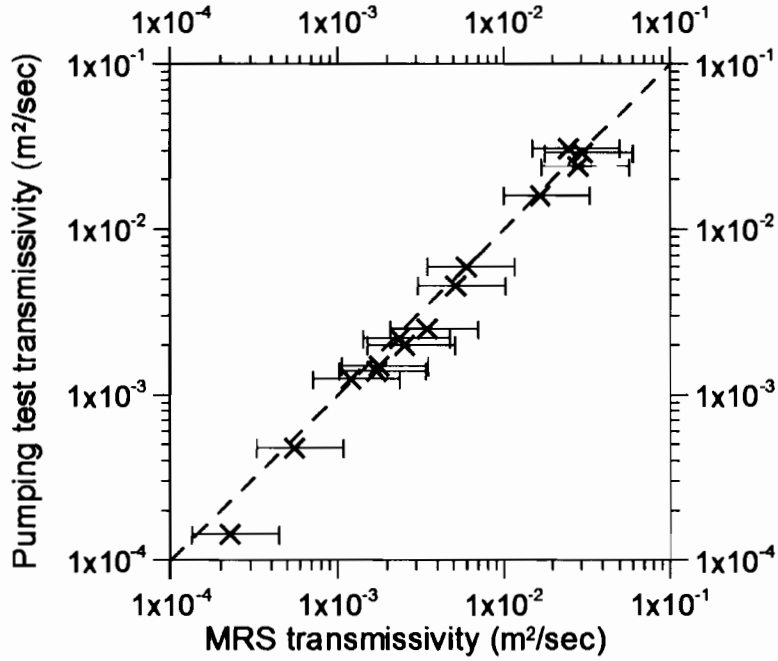

Figure 5. Comparison of MRS transmissivity estimation with that given by pumping tests.

In conclusion, we need to discuss the principal limitation of the applicability of MRS to non-invasive estimation of the permeability.

Hydraulic permeability of geological formations is scale-dependent. Samples investigated in laboratories, using borehole NMR tools or performing MRS measurements all have very different scale. Thus, results obtained with these methods might be different. An example of two aquifers of different type is presented in Figure 6.

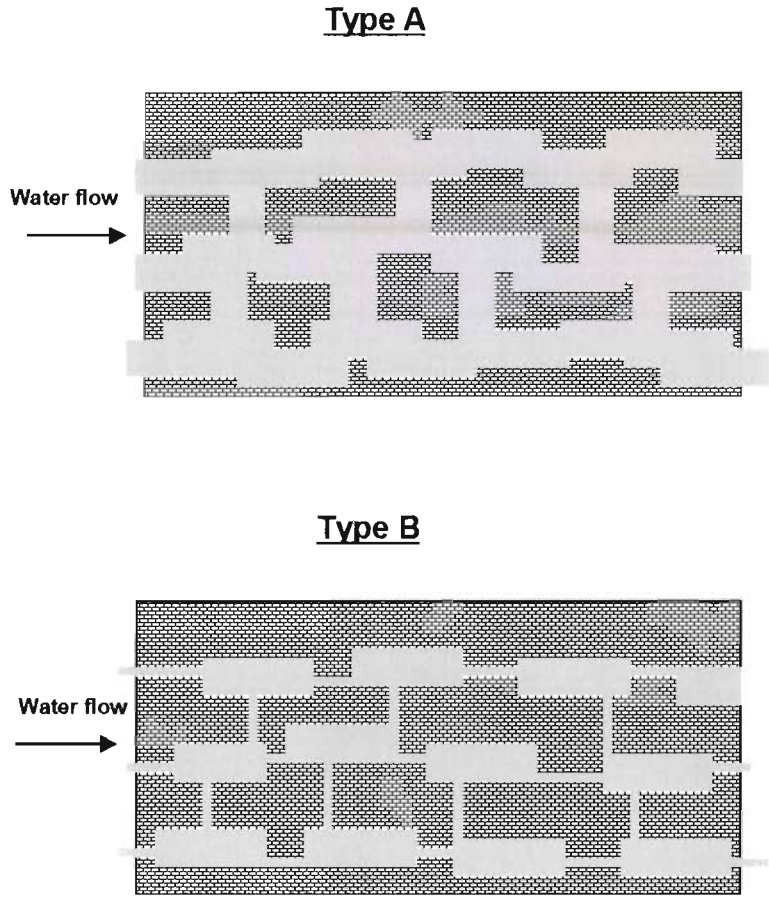

Figure 6. Permeability of aquifers : type A – single porosity; type B – double porosity.

In aquifer with a single porosity (type A), the water is located in similar pores and permeability of this aquifer is closely related to the pore size. In this case, information about the aquifer derived from magnetic resonance measurements is also related to permeability even if investigated samples are of a different volume.

In aquifer with a double porosity (type B) shown in Figure 6, most of the water is located in large pores, but permeability mostly depends on small pores. In this case, if the volume of investigated sample is small (lab. measurements), result of permeability estimation depends on whether the selected sample represents small or large pores. A large-scale method like the MRS will provide us with information mostly related to

large pores, as they contain larger quantity of water than small pores. Obviously, the permeability estimation is much less accurate in this case.

In practice, different types of porosity are usually mixed, and measured magnetic resonance signal is often composed of a sum of signals decaying with different relaxation times and thus, contains information about different pores.

1.2. THE DEPTH OF INVESTIGATION

The magnetic resonance signal is sensitive to different natural factors what makes the performance of the method site-dependent. The most common and practically important variations in the magnetic resonance signal are related to the natural geomagnetic field and the electrical conductivity of rocks (Semenov, *et al.*, 1989; Shushakov, 1996; Legchenko, *et al.*, 1997; Valla and Legchenko, 2002). The electrically conductive subsurface attenuates alternative electromagnetic fields by a factor characterized by the "skin depth" that is proportional to $\sqrt{\rho/f}$, where ρ is the resistivity of the subsurface, and f is the frequency of the electromagnetic field. The Larmor frequency used in MRS is proportional to the geomagnetic field magnitude $f_0 \sim H_0$. Consequently, in areas with a low geomagnetic field (towards the equator), the frequency is smaller, and the attenuation caused by the subsurface is less important than in areas with a high geomagnetic field (towards the poles). However, the magnetic resonance response is proportional to square of the geomagnetic field ($E \sim H_0^2$), what improves the signal to noise ratio in areas with a high geomagnetic field even taking into account the

attenuation caused by the subsurface. The inclination of the geomagnetic field also modifies the magnetic resonance signal (Legchenko, *et al.*, 1997). A numerical demonstration of influence of these natural factors on the maximum depth of investigation of the MRS method is presented in Figure 7. The maximum depth of detection of a one meter thick infinite horizontal layer of water (100% of the water content, and T_2^*=1000ms) in a noiseless environment is depicted versus the half-space resistivity. Calculations were performed for different geomagnetic fields using NUMIS^{PLUS} standard configuration: a square loop with a side of 100 m, a signal detection threshold of 10 nV, and a maximum pulse of 12000 A-ms. We can see that magnitude and inclination of the geomagnetic field is a major factor that defines MRS performance when the subsurface is non-conductive. Influence of electrically conductive layers becomes important when the resistivity of these layers is less than 50 ohm-m approximately.

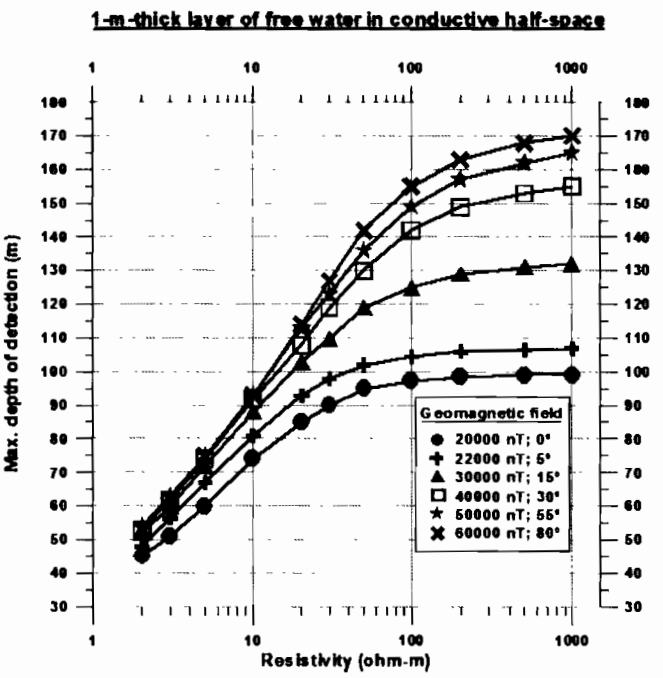

Figure 7. The maximum depth of detection calculated for a 1-m-thick layer of free water (w=100%) versus the half-space resistivity.

Inversion of MRS data ($E_{0d}(q)$ and $T_2^*(q)$), provides the depth (z), the thickness (Δz), the water content (w), and the relaxation times T_2^* and T_1 for each water-saturated layer. However, like many other geophysical problems, the MRS inverse problem is ill-posed and therefore the solution is non-unique (Legchenko and Shushakov, 1998). We present "smooth inversion" results performed following the Tikhonov regularization method, but other methods like the linear programming and Monte Carlo inversion could also be used (Guillen and Legchenko, 2002; 2002a).

The resolution of the MRS method decreases with increasing depth. In order to demonstrate the MRS vertical resolution against the depth, we compute MRS signals from an inclined 10-m-thick water-saturated layer that is shown in Figure 8. We assume that soundings are performed along a profile from the deepest part of the layer toward the shallow part. Results of 1D inversion for the water content (w), and for the relaxation time (T_2^*) are plotted versus the distance (Figure 9). The dashed lines in the plot show the model. We can see that the resolution degrades progressively with increasing depth. While the top of the layer (z) is relatively well resolved down to 100 m, the thickness of the layer is still resolved down to about 60-70 m. Below 70 meters the thickness (Δz) and the water content (w) can not be derived from MRS data. The relaxation time (T_2^*) is well resolved down to 100 m for this model.

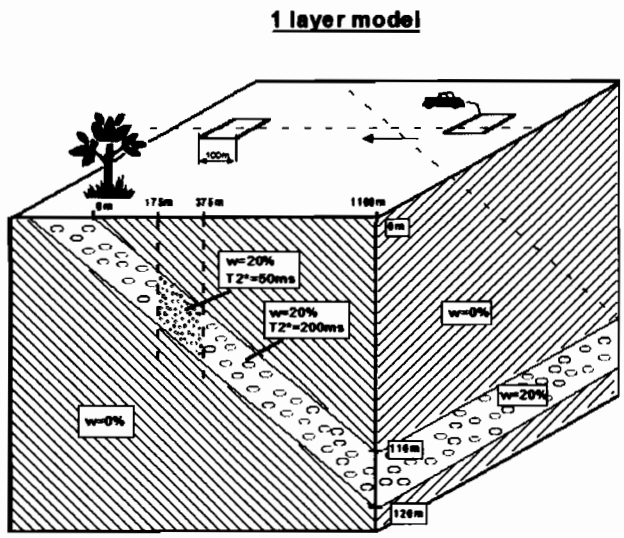

Figure 8. One layer model.

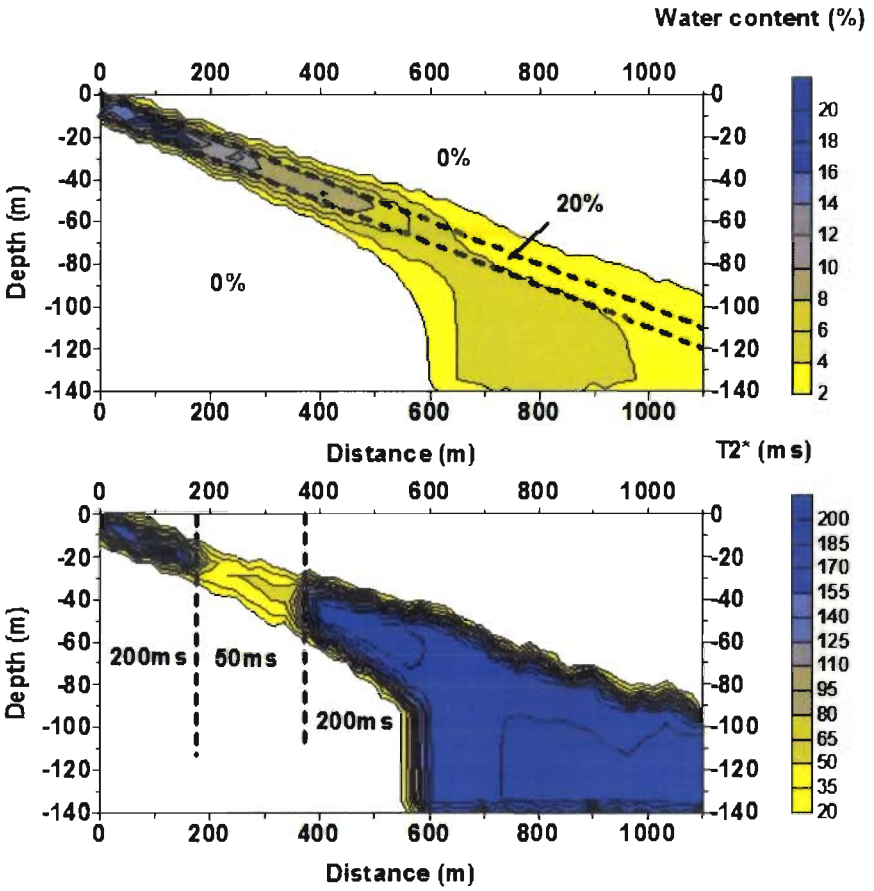

Figure 9. Resolution of the one layer model.

1.3. EXAMPLE OF MRS RESULTS

Example of MRS results obtained in France is presented in (Figure 10). Investigated aquifer is composed essentially of medium to coarse sand. Field measurements were carried out near a borehole where the pumping tests were fulfilled.

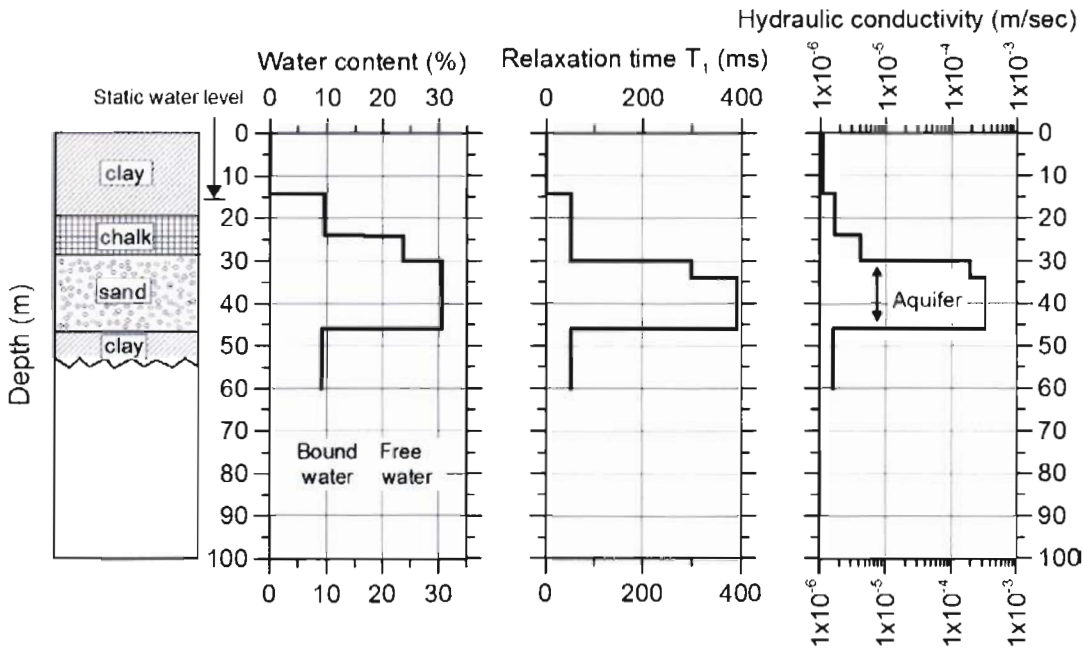

Figure 10. Example of MRS results.

Increase in the water content observed in the MRS log corresponds to the water table indicated by borehole. However, the relaxation time corresponding to this zone is short ($T_1 \approx 50ms$). It means that the permeability of the rock between 15 and 30 meters is low and that most of the water is capillary-bound water. Increase in the relaxation time corresponds well to top of the aquifer indicated by the lithological log. The MRS permeability estimation also shows that the top of the aquifer is about 15 m below the

water static level. A good agreement between the transmissivity estimated by MRS ($T_{MRS} = 4.7e-3(m^2/\sec)$), and that derived from pumping tests ($T_{bh} = 4.6e-3(m^2/\sec)$) is observed. Unfortunately, lack of data about the effective porosity does not allow us to calibrate the MRS water content.

1.4. NUMIS^{PLUS} MRS EQUIPMENT

The NUMIS ^{PLUS} instrument consists of an oscillating-current generator, a receiver, a PMR signal detector, an antenna and a microprocessor (Figures 11, 12). The antenna is used for both transmission of the oscillating magnetic field and reception of the PMR signal. The microprocessor switches the antenna from generator to receiver mode by an electronic switch. It also controls the generation of the reference frequency equal to the Larmor frequency. An envelope of the signal from the phase-sensitive detector is recorded by the microprocessor in digital form. A portable PC is used for data processing. The PC is connected to the microprocessor by a standard RS-232 serial link.

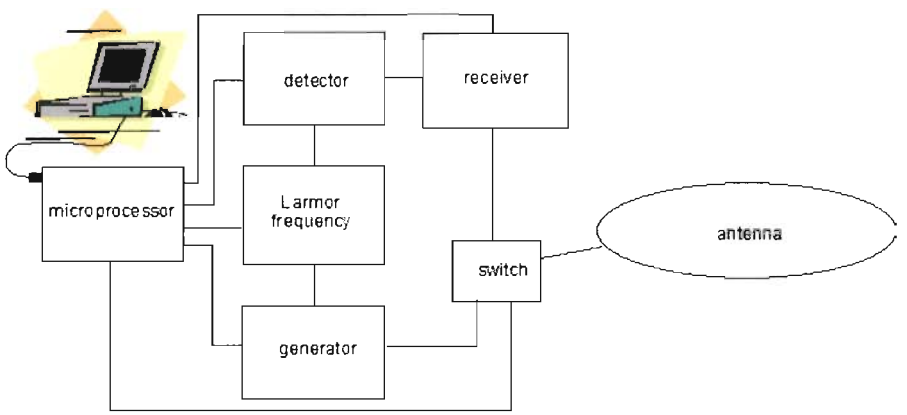

Figure 11. Scheme of NUMIS^{plus} instrument.

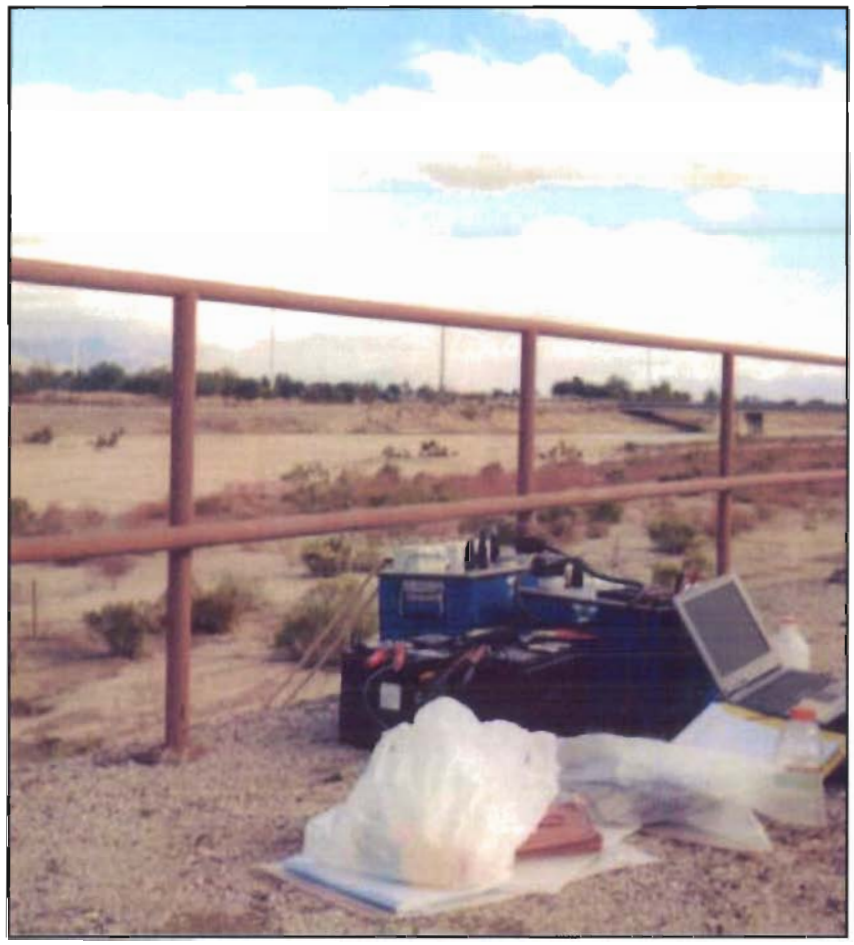

Figure 12. NUMIS^{plus} equipmen in a field.

1.5. OUTPUT OF NUMIS^{PLUS} SYSTEM

The data interpretation software developed for NUMIS^{plus} system is very flexible and provides to users a wide range of possibilities to configure the output page. In this report, the configuration presented in Figure 13 is used.

Site: haddam meadows profile, sounding 7
Loop: 4 - 37.5 Date: 18.11.2000 Time: 13:13
NUMIS data set: C:\moi\REPORTS\usa2002\interpr\Haddam_Meadows\Haddam_Meadows-2000\HM7.inp
matrix: C:\moi\REPORTS\usa2002\interpr\Haddam_Meadows\MATRIX\Had_mead-8sq.mrm
loop: eight square, side = 37.5 m
geomagnetic field:
inclination= 72 degr, magnitude= 53399.06 nT

filtering window = 198.7 ms
time constant = 15.00 ms
average S/N = 2.89; EN/IN = 1.46
fitting error: FID1 = 17.06%; FID2 = 34.19 %
param. of regular.: modeling
permeability constant Cp = 7.00e-09

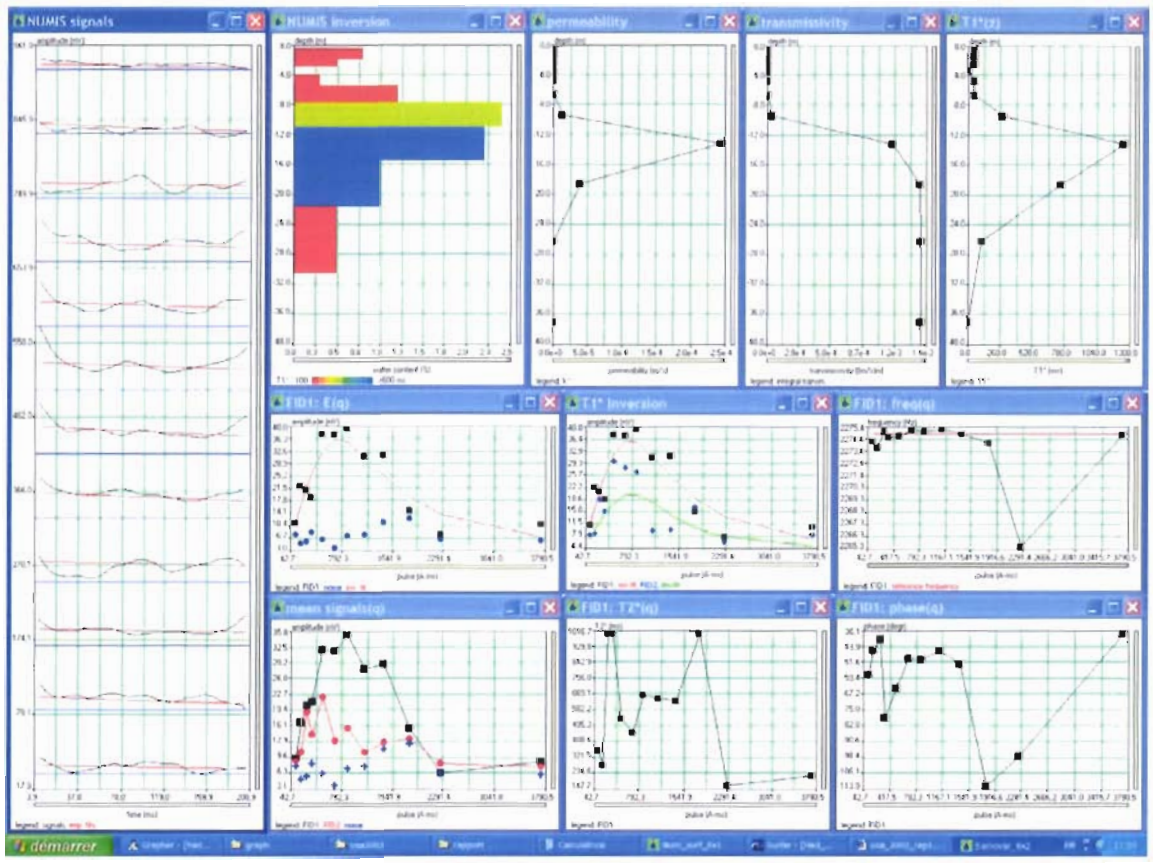

Figure 13. Example of NUMIS^{plus} output page.

MRS results are presented by following graphs:

1) **NUMIS signals** - free induction decay signals after the first pulse (FID1) and inversion fits versus the time are arranged by increasing pulse parameter from the bottom to top.
2) **NUMIS inversion** – vertical distribution of the water content with the relaxation time T_1 presented by the color scale.
3) **Permeability** – MRS estimation of the permeability versus depth.
4) **Transmissivity** - MRS estimation of the transmissivity versus depth.
5) $\mathbf{T_1^*(z)}$ - vertical distribution of the relaxation time T_1.
6) **FID1: E(q)** – amplitude of the FID1 signal, inversion fit and an average noise versus the pulse parameter.
7) $\mathbf{T_1^*}$ **inversion** – amplitude of the FID1 and FID2 signals and the inversion fit.
8) **FID1: freq(q)** – the Larmor frequency measured after the first pulse.
9) **Mean signals(q)** – average through the data acquisition window signals (FID1 and FID2) and the noise.
10) **FID1:** $\mathbf{T_2^*(q)}$ - relaxation time T_2^* versus the pulse parameter.
11) **FID1: phase(q)** – phase of the signal measured after the first pulse.

In the header, information about parameters used for the interpretation is presented.

1.6. NUMIS^{PLUS} DATA: QUALITY ESTIMATION

Currently, the MRS method is able to detect water in aquifers composed of non-magnetic rocks. The magnetic resonance signal may vary from 0 to about 4500 nV (4.5e-6 V). Typical range for Europe is 0 – 500 nV, but for igneous rocks it is 0 – 150 nV. NUMUS^{plus} instrument has an instrumental noise of about 3-5 nV what puts the

threshold of reliable measurements of magnetic resonance signal to 5-10 nV approximately.

For MRS data quality estimation, the following parameters can be used:

1) External noise level after stacking and filtering is compared with the NUMIS instrumental noise as

   $$EN / IN = (ext.noise) / (instr.noise) = noise / 5 . \qquad (21)$$

   In ideal case, when the external noise is very small, the EN/IN ratio is about equal to 1. When the magnetic resonance signal is very small, the stacking should be carried out until $EN / IN \cong 1$. When $EN / IN \cong 1$ the sounding can be considered as of a good quality, even if the signal has not been detected.

2) The signal to noise (observed noise includes both external and instrumental noises) ratio

   $$S / N = signal / noise . \qquad (22)$$

   Usually data are considered of a good quality when S/N>2. In this case, a quantitative interpretation of MRS data is possible, and reliable information about aquifers can be derived from MRS data. When S/N>2, it is not necessary to have $EN / IN \cong 1$.

   If $EN / IN \cong 1$ and S/N=1 (signal is not detected), a quantitative interpretation of MRS data is not possible. However, it can be concluded that there is no water (detectable by MRS) in the subsurface. Approximately, the threshold of the detectable water content for NUMIS instrument is about 0.5-1%.

   When $EN / IN > 1$ and S/N=1, the sounding cannot be considered as of a good quality. The only conclusion can be derived from the data is that the amplitude of MRS signal is smaller than the noise level. For example, if $EN / IN = 5$ and S/N=1, one can conclude that the signal is smaller than 25 nV.

3) The frequency of the MRS signal must be stable and close to the Larmor frequency given by a proton magnetometer. The difference in-between is usually less then 3-4Hz.

4) The phase of the MRS signal must be stable or vary smoothly. The phase helps for discrimination between the MRS signal (phase is stable or vary smoothly) and a cultural noise: the frequency of a cultural noise might stable (but not necessary close to the frequency given by a proton magnetometer) but the phase of noise is always random.

5) The relaxation time $T_2^*(q)$ is the parameter the most sensitive to data quality.

   For data of a good quality $T_2^*(q)$ is stable or varies smoothly between 50 and 400ms.

When quantitative interpretation of MRS measurements is not possible, an estimation of the maximum possible volume of water per surface unite can be made:

$$V_{MRS} = \int_{\Delta z} w(z)dz \,. \qquad (23)$$

V_{MRS} can be used when large-yield-aquifers is a target and caracterization of small aquifers is out of scope of survey. In this case, just achieving $V_{MRS} < V_{MRS}^{limit}$, where V_{MRS}^{limit} is considered as a limit for an acceptable aquifer for the investigated area, sounding can be stopped without spending more time in the field.

2. Test sites

In this report, we present three areas in northern Denmark where MRS method was tested. Five MRS stations along a profile in Hogsted area, one station in Saby and one station in Nosby were carried out. Transient EM measurements were performed at all MRS stations.

No detailed geological description of the test sites is available for writing this report. According to general information, the subsurface is composed of rather heterogeneous glacial deposits. The hydrodynamic properties of this material vary a lot and aquifers of interests are essentially located in ancient valleys. However, even in the valleys rocks may have very low permeability what makes the knowledge about the location of these valleys not sufficient for reliably implantation of water supply wells.

2.1. SABY AREA

Location of MRS station in Saby area is presented in Figure 14.

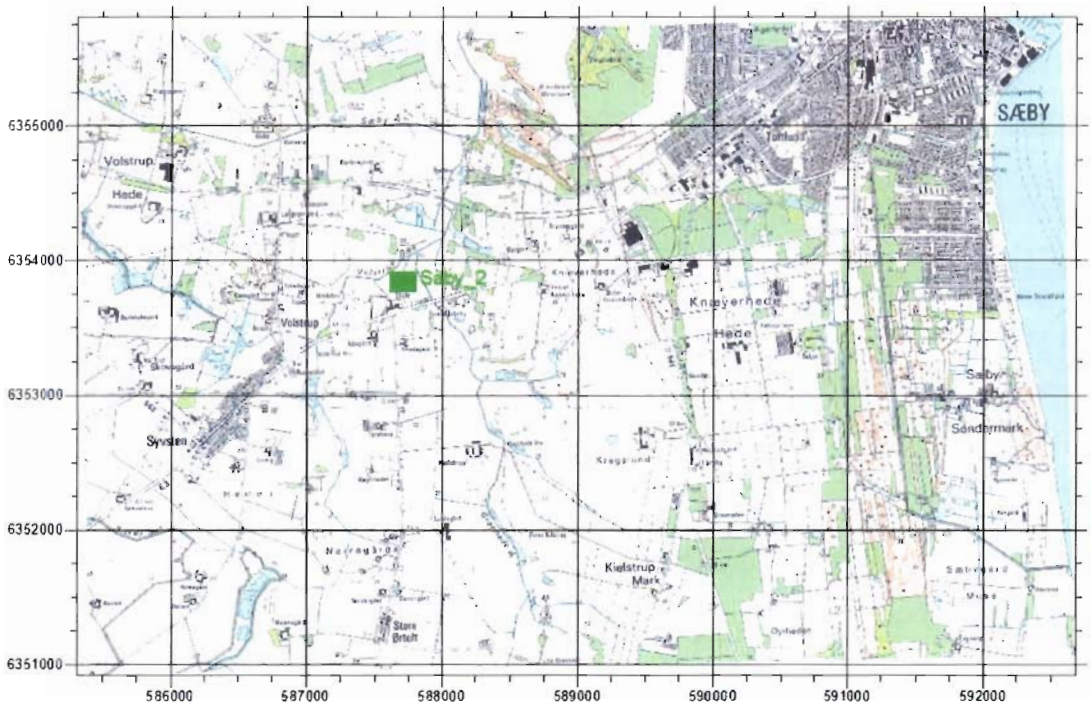

Figure 14. Location of the MRS station in Saby area.

2.2. NOSBY AREA

Location of MRS station in Nosby area is presented in Figure 15.

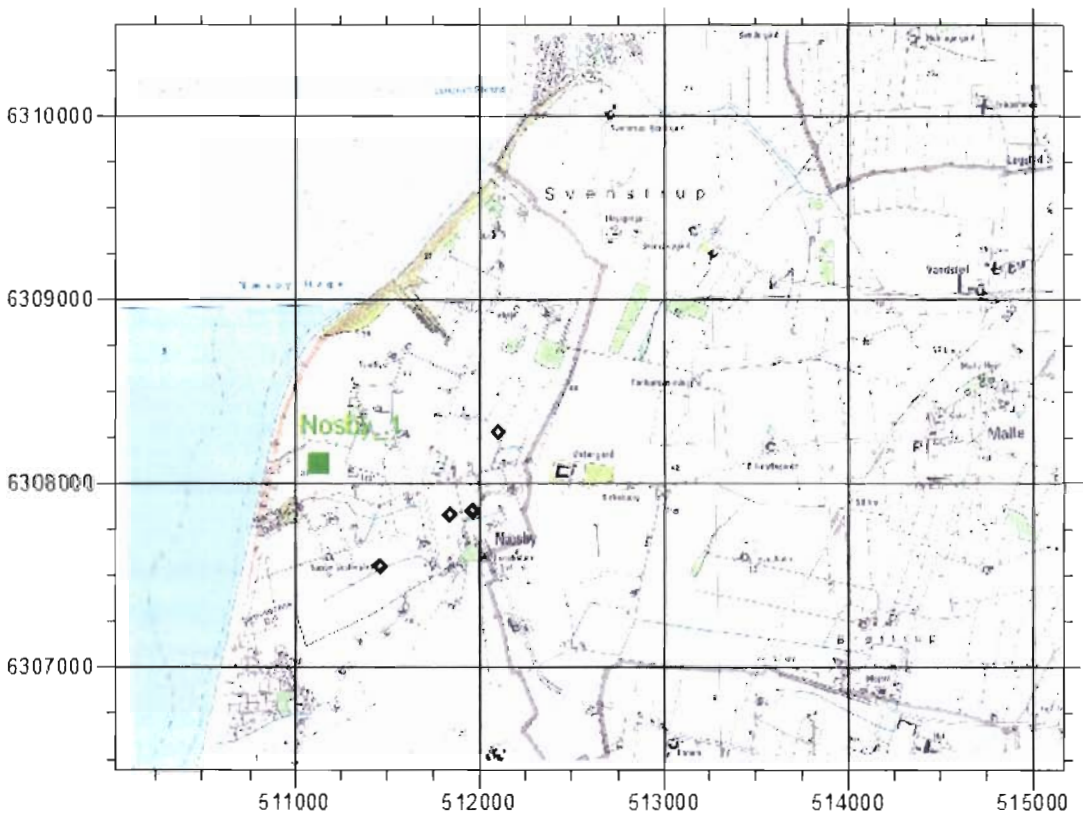

Figure 15. Location of the MRS station in Nosby area.

2.3. HOGSTED AREA

Location of MRS stations in Hogsted area is presented in Figure 16.

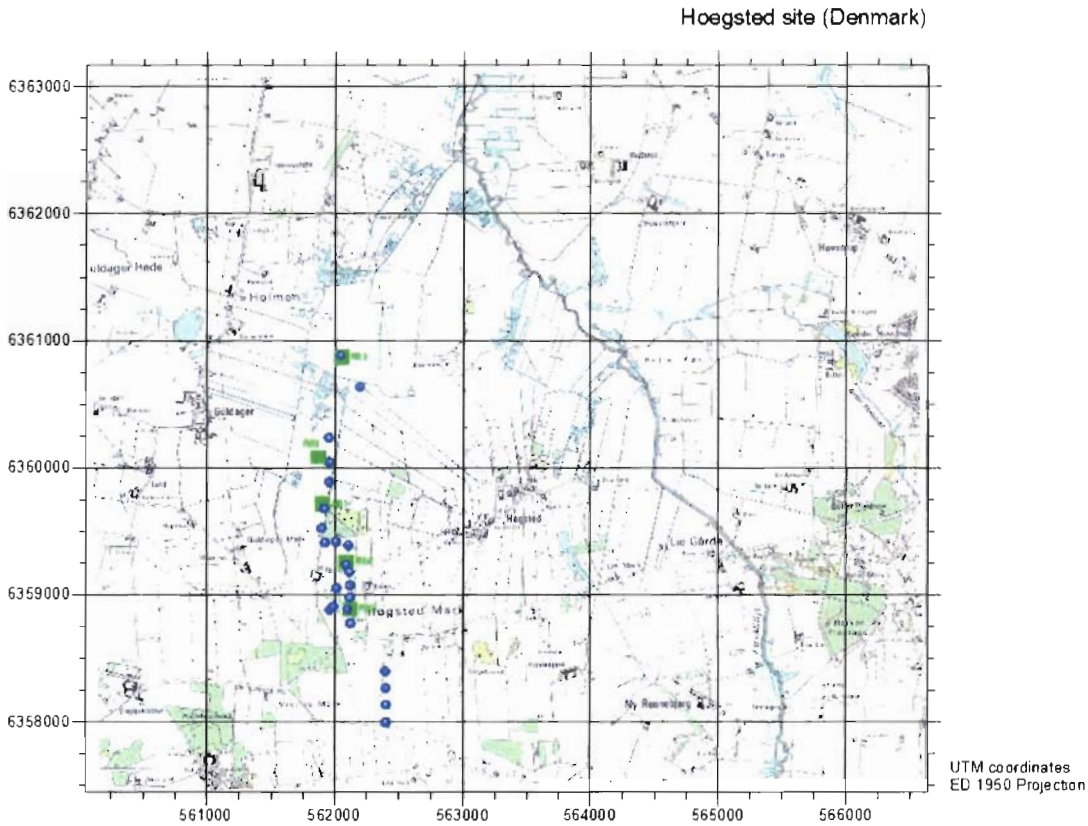

Figure 16. Location of MRS stations in Hogsted area (R01-R05).

3. Results and discussion

3.1. SUMMARY

Totally, 7 soundings are presented in this report. All MRS measurements were carried out using NUMIS^{plus} instrument manufactured by IRIS Instruments. The data processing was performed using NUMIS standard interpretation software. The electrical conductivity of rocks was not taking into account. The subsurface was considered as a 100 ohm-m half-space. The depth of MRS investigation depends on the antenna size. With the square loop of 75-m-size used for all soundings the depth of investigation is about 100 meters.

Results of NUMIS data interpretation are presented in Annexes 1.

GPS co-ordinates and estimation of the quality of MRS data are presented in Table 2.

MRS Station	T_Easting	T_Northing	EN/IN	S/N	Signal	Interpretation
Saby	587918,1	6354191,6	13.7	0.99	No	Qualitative
Nosby	511063,8	6308095,0	26.8	0.8	No	Qualitative
Hogsted_1	561894,0	6359716,8	15.5	1.58	Yes	Quantitative
Hogsted_2	562115,4	6358884,7	11.9	1.57	Yes	Qualitative
Hogsted_3	562047,8	6360865,5	7.1	2.1	Yes	Quantitative
Hogsted_4	562085,6	6359255,1	29.4	1.2	Yes	Quantitative
Hogsted_5	561933,5	6360127,7	28	3	Yes	Quantitative

Table 2. GPS co-ordinates and quality of MRS data.

During the survey a very high level of industrial noise was observed. As the depth of investigation of at least 80 meters was required, application of eight-shape-loop of 37-m-side which allows improving S/N at the factor of about 10 and is a standard setup for NUMIS system was excluded. Unfortunately, sufficient amount of wire was not foreseen in the beginning, and thus application of larger eight-shape-loop (75-m-side) for investigating greater depth was not possible. Quality of data necessary for reliable

interpretation of MRS measurements was achieved by using the notch-filtering and great number of stacks (500). With 500 stacks one sounding takes about 10 hours. Even time-non-efficient, this setup allows answering to the principal question about the applicability and geophysical efficiency of MRS in Denmark.

When the MRS signal is detected (5 soundings), a quantitative interpretation of MRS data reveals the geometry, water content, and permeability of aquifers. In two cases the magnetic resonance signal was not detected. A qualitative interpretation reveals only an estimation of maximum possible MRS water volume inside of the loop area. This estimation only guarantees that it is not possible to have more water than is given by the maximum possible volume. However, it is also possible that there is no water at all at this site.

For example, MRS amplitudes measured at all seven test sites in Denmark are presented in Figure 17. It can be seen that the MRS signal is smaller for the sites Saby 2, Nosby and Hogsted 2 and thus, a poor signal to noise ratios for these sites can be explained by not much higher noise, but smaller signals. After our experience, in the subsurface composed of glacial deposits smaller signals are often associated with compact low permeable silt/clay-type material.

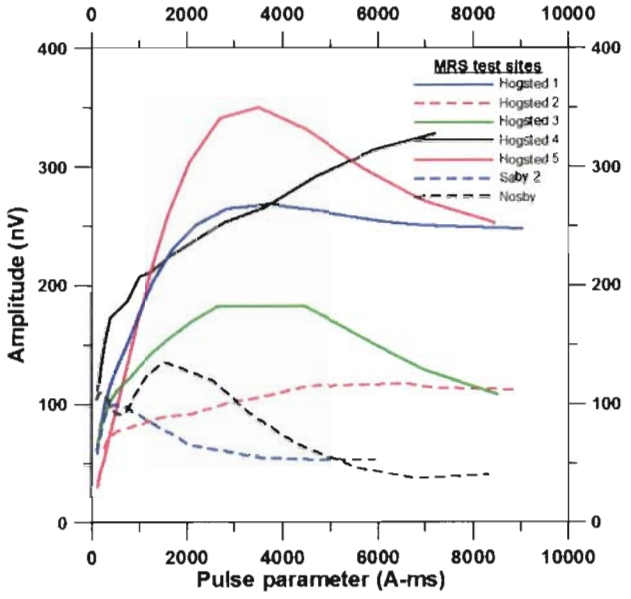

Figure 17. Comparison of MRS amplitudes.

Summary of MRS results in Denmark is presented in Table 3.

MRS Station	*Top (m)*	*Bottom (m)*	V_{MRS} *(m³/m²) (<100m)*	T_{MRS} *(m²/s) (<100m)*	k_{MRS} *(m/s)*	Comments
Saby	6	18	<0.2	-	-	Insufficient S/N.
Nosby	16	36	<0.9	-	-	Insufficient S/N.
Hogsted_1	20	>100	>8.8	$>4x10^{-3}$	Shallow: $1.2x10^{-4}$ Deep: $2x10^{-5}$	Thickness is not defined. Significant contribution of shallow aquifer.
Hogsted_2	36	>100	<2.4	$<6x10^{-4}$	$<1x10^{-5}$	Thickness is not defined.
Hogsted_3	25	55	2.2	$2x10^{-3}$	$1.1x10^{-4}$	Only shallow aquifer is detected.
Hogsted_4	45	>100	>8	$>6x10^{-3}$	$1.4x10^{-4}$	Thickness is not defined.
Hogsted_5	25	>100	>9	$>6x10^{-3}$	Shallow: $1.7x10^{-4}$ Deep: $4x10^{-5}$	Thickness is not defined. Major contribution of shallow aquifer.

Table 3. Aquifers detected by MRS in Denmark.

With NUMIS setup which was used during the survey in Denmark, the maximum depth of investigation is about 100-120 meters, but quantitative results can be obtained down to 80 meters approximately. For this reason quantitative characterization of thick aquifers between 60 and 160 meters is limited by the depth of 80, possibly 100 meters.

As we have no experience in MRS application in Denmark, we do not know whether there is a correlation between the hydrodynamic properties of glacial material for shallow (first 100 m) and deep parts of ancient valleys (between 100 and 200 m). If such a correlation does exist, then after MRS results it can be concluded that all the investigated during this survey aquifers are composed of rather fine material and cannot be recommended for implantation of high-yield-wells for the water supply. If more coarse material may exist below 100 meters, then nothing can be said about rocks between 100 and 200 meters.

3.2. SABY

Data are of poor quality ($EN/IN = 13.7$), and no signal was detected ($S/N \cong 1$, frequency and phase are unstable). Aquifers cannot be reliably characterized in this case. Only estimation of maximum possible volume of water can be done (Table 3). MRS log is presented in Figure 18.

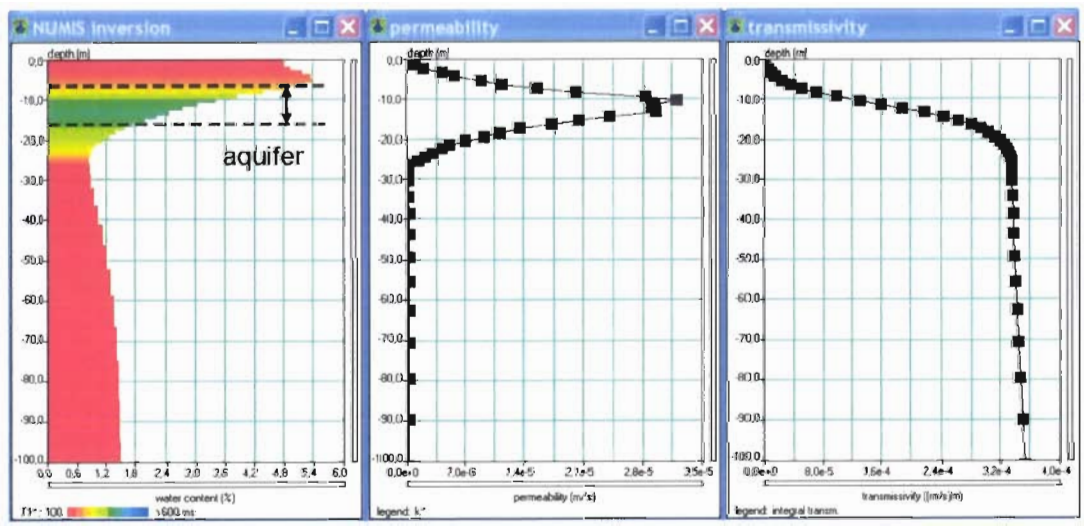

Figure 18. MRS log in Saby.

MRS provides only qualitative information about absence of aquifers that could be used for water supply purposes down to about 80-100 meters.

3.3. NOSBY

Data are of poor quality ($EN/IN = 26.8$), and no signal was detected ($S/N \cong 1$, frequency and phase are unstable). Aquifers cannot be reliably characterized in this case. Only estimation of maximum possible volume of water can be done (Table 3). MRS log is presented in Figure 19.

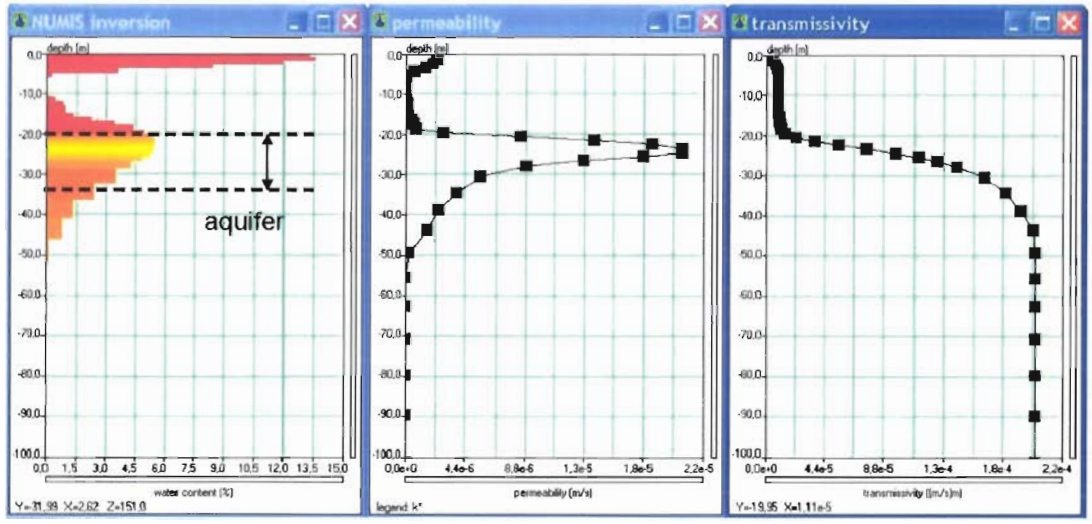

Figure 19. MRS log in Nosby.

Because of field-time for working in this area was limited, number of stacks that would be sufficient for achieving the necessary quality of data for quantitative characterization of aquifers has not been implemented. Consequently, MRS provides only qualitative information about absence of aquifers that could be interesting for water supply purposes down to about 80 meters.

3.4. HOGSTED

Five soundings along the profile were performed in Hogsted area. Location of MRS stations is shown in Figure 16. Quality of the data allows characterizing aquifers quantitatively (Table 2).

Large variations in the amplitude of the magnetic resonance signal along the MRS profile were observed (Figure 20). These variations can be explained by lateral in-homogeneities of the subsurface.

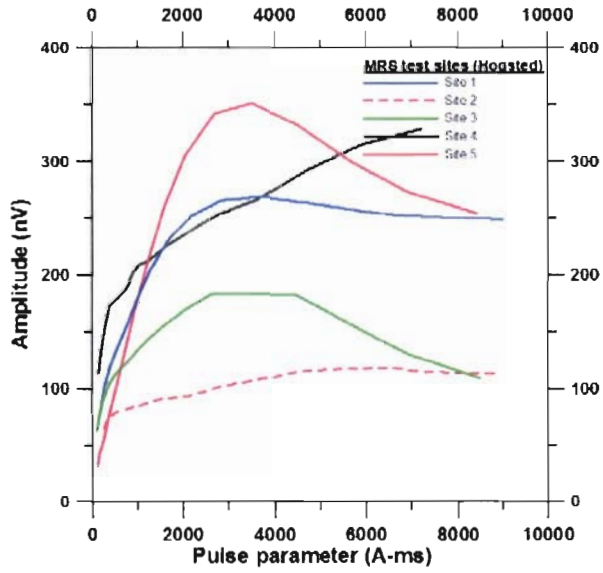

Figure 20. Amplitude of MRS signals in the Hogsted area.

MRS logs in Hogsted area are presented in Figures 21-25.

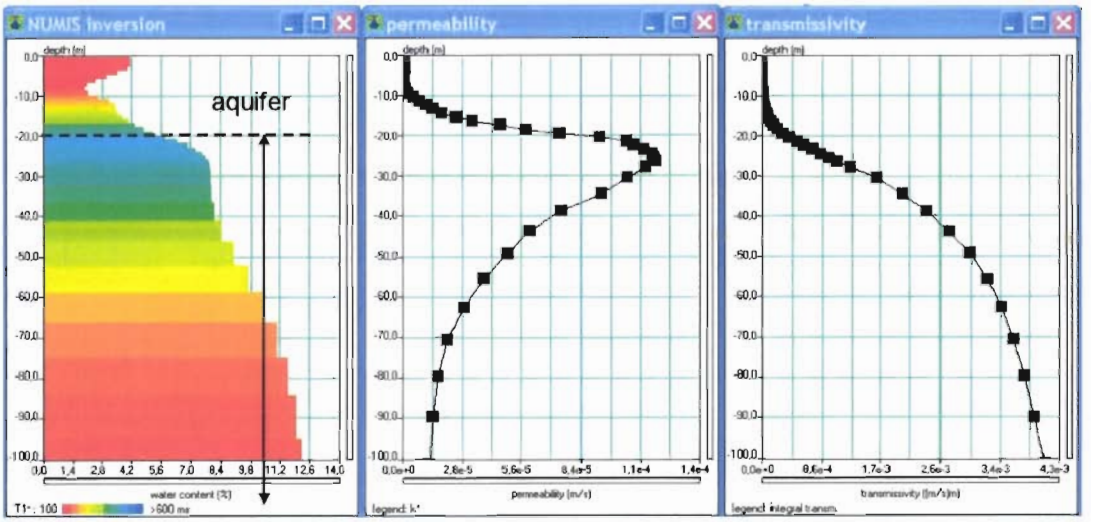

Figure 21. MRS log in Hogsted, Site 1.

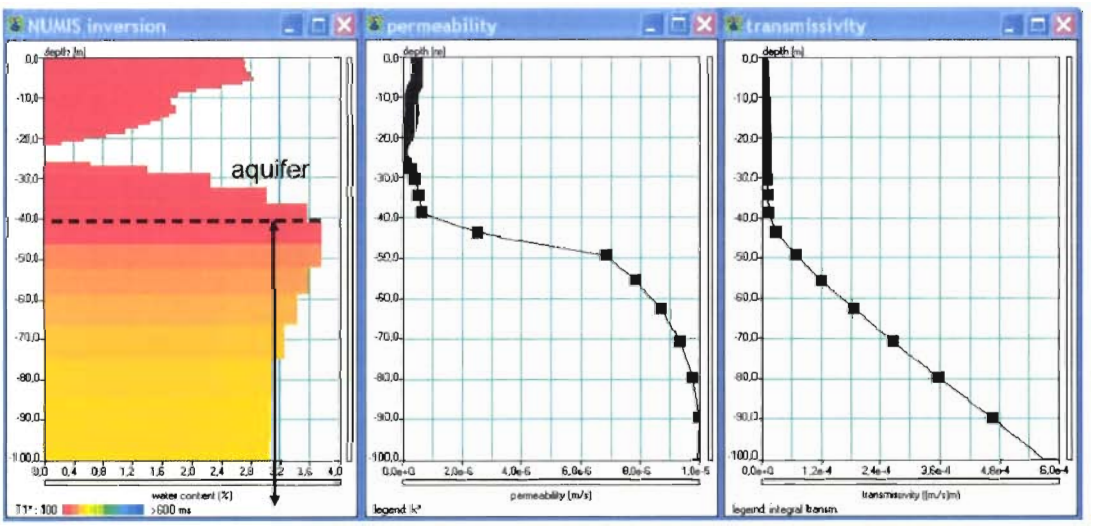

Figure 22. MRS log in Hogsted, Site 2.

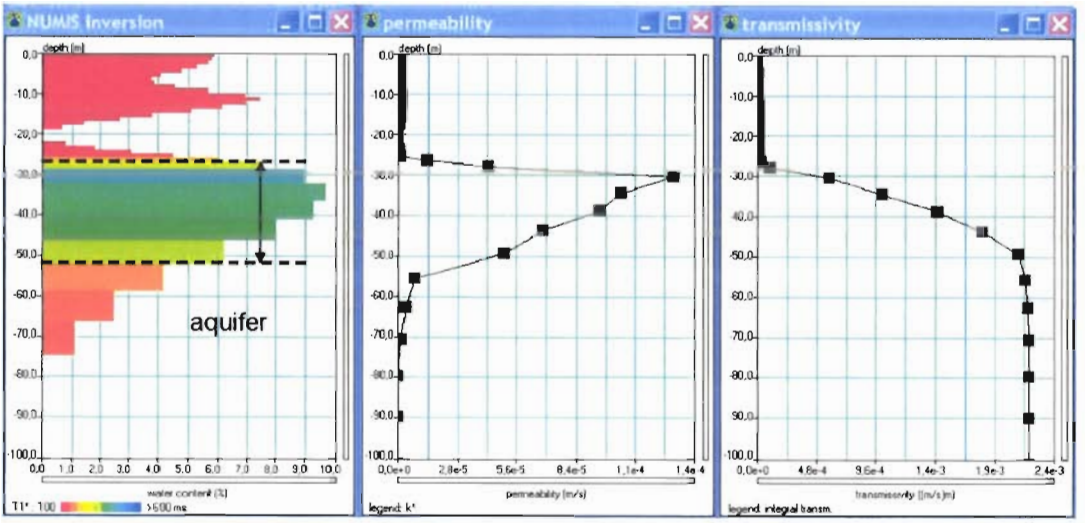

Figure 23. MRS log in Hogsted, Site 3.

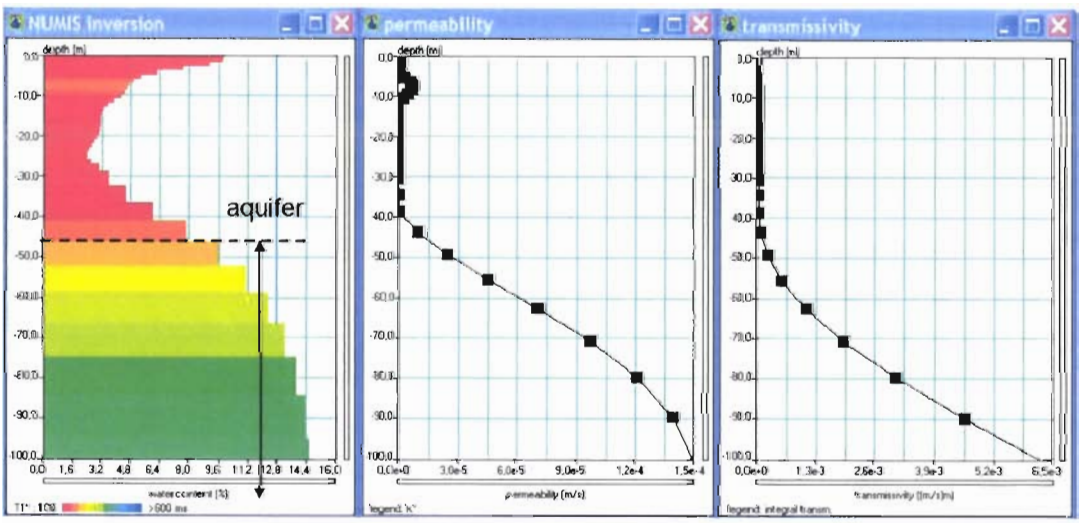

Figure 24. MRS log in Hogsted, Site 4.

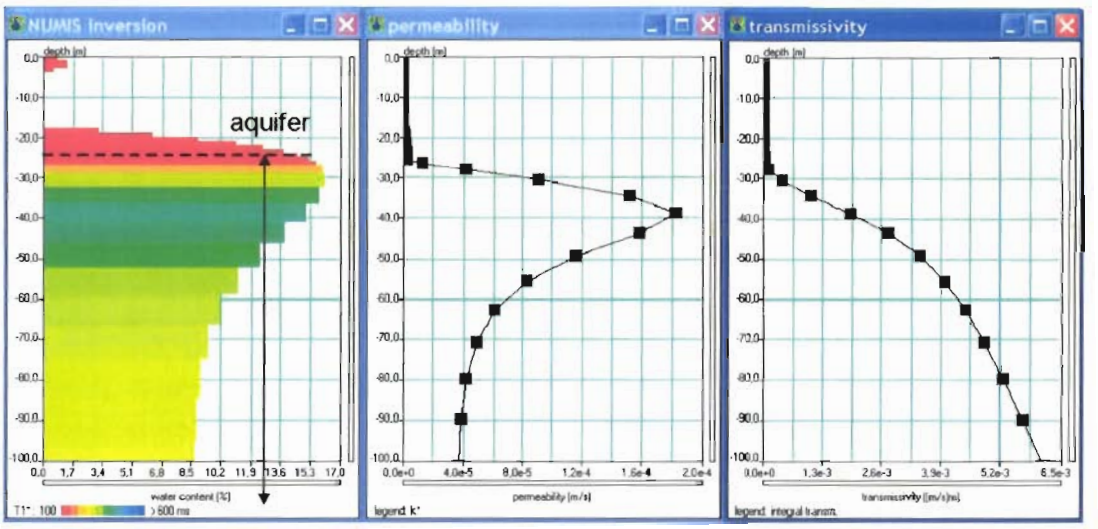

Figure 25. MRS log in Hogsted, Site 5.

The water content and the permeability cross-sections derived from MRS data along the profile in Hogsted are presented in Figure 26.

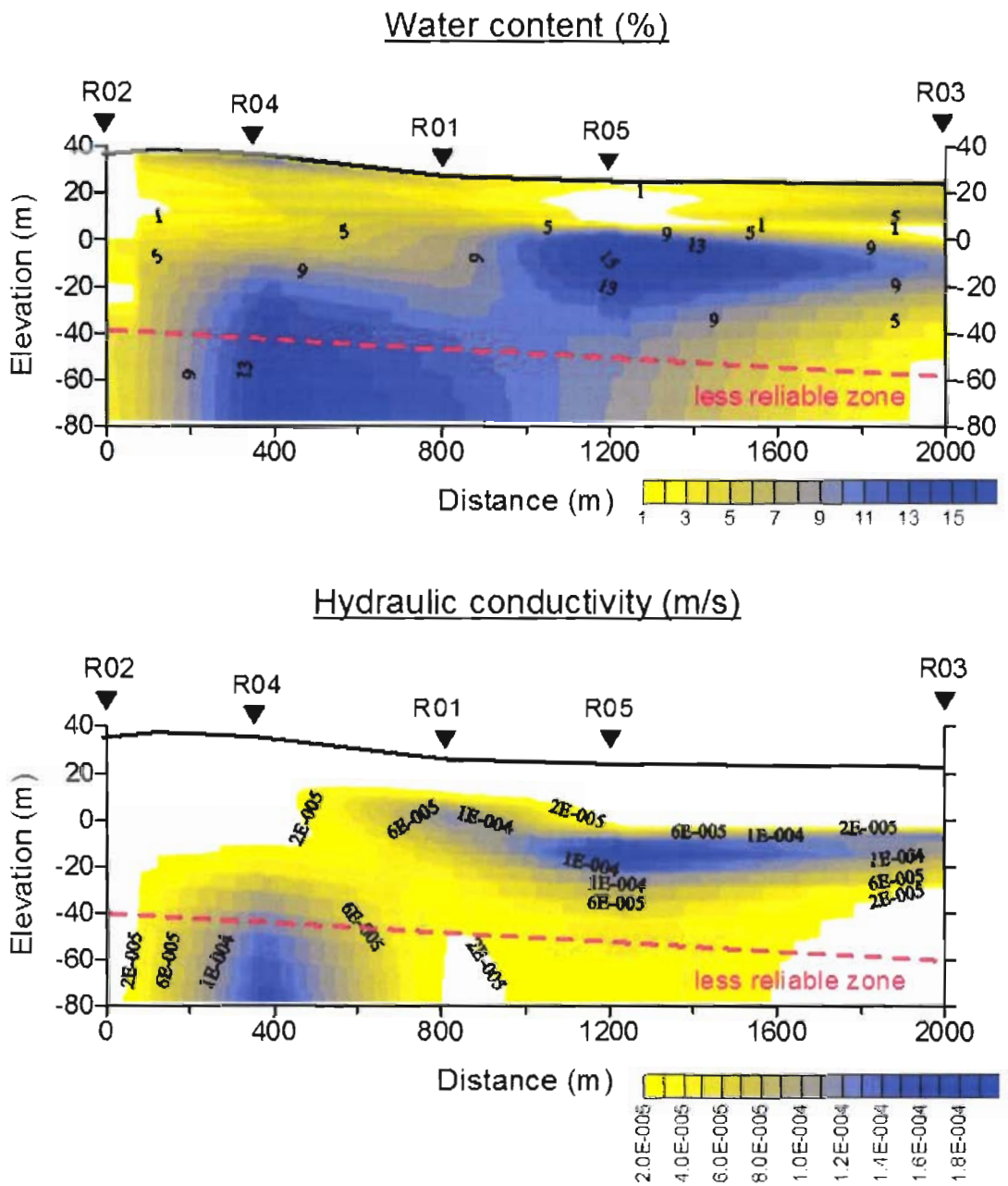

Figure 26. MRS cross-sections in Hogsted area.

Two aquifers are detected by MRS. A shallow aquifer at a depth between 20 and 50 meters (MRS stations 1, 3, 5). The permeability of this aquifer is varying along the profile and has the maximum at the Site 5. A deep aquifer, which is probably corresponding to an ancient glacial valley, is detected by stations 1 and 4. Station 2 shows that this deep aquifer is not continuing towards the north. As the depth of investigation is not sufficient for reliable characterization of this deep aquifer, one should be careful for when selecting the location for drilling between MRS stations 1, 4 and 5. For that, we would recommend to use more geological and probably geophysical information about this area.

MRS users should be aware that MRS is not able to identify rocks. It is only estimating the water content (through the amplitude of the MRS signal) and the mean size of pores (through the relaxation time of the signal). However, using the experience from other surveys and the knowledge that the subsurface is composed of glacial materials, we can propose a possible geological interpretation. We assume deposits with very low permeability as the "till", more permeable parts of the subsurface as the "very fine sand", "fine sand" and "fine to medium sand".

Proposed geological interpretation of the MRS results along the profile in Hogsted area is presented in Figure 27.

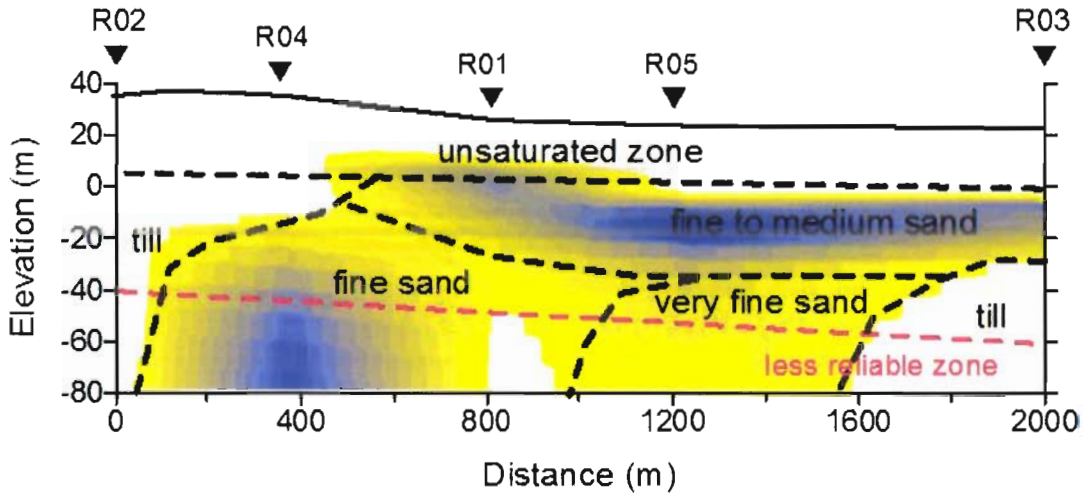

Figure 27. Possible geological interpretation of MRS results along the profile in Hogsted area.

Conclusions

Very high level of manmade noise was observed during this survey. However, our conclusion is that NUMIS system may be efficient when optimized to these conditions. After two-weeks experience in northern Denmark, the main conclusion can be made that the MRS method works well and, especially for the first 100 meters of the subsurface, is a useful geophysical tool for groundwater investigation.

Totally 7 MRS stations were investigated in northern Denmark in August 2003. Five measurements in Hogsted area were carried out along a 2-km-long profile. One measurement was performed in Saby and one in Nosby areas.

In Saby and Nosby, the magnetic resonance signal was not detected. In both cases, MRS cannot be used for the quantitative characterization of the subsurface. However, the insufficient for quantitative interpretation signal to noise ratio can be explained not only by very high noise, but also by small signals. Thus, it can be concluded that for the first 80-100 meters of the subsurface no major aquifers that can be used for water supply purposes exists at investigated sites.

In Hogsted area MRS results provide quantitative information about aquifers: geometry and estimation of hydrodynamic properties (MRS estimation of the water content and hydraulic conductivity). Two aquifers are detected in this area. The shallow aquifer between 20 and 50 meters is composed of a rather permeable material, possibly of fine to medium sand ($k \approx 2 \times 10^{-4}$ m/s); and it can be used for implantation of water supply wells. The deep aquifer, which may correspond to an ancient glacial valley, is composed of a material with a relatively low permeability ($k < 1 \times 10^{-4}$ m/s). As the depth of investigation by MRS was limited by NUMIS setup to 80-100 meters, the thickness of this aquifers and its permeability in the deepest part cannot be estimated. Basing on our experience outside of Denmark we expect a relatively small yield and would not recommend drilling a water supply well in such a material. However, taking

into account that this aquifer is about 100-m-thick, other data (if available) and experience in local environment may help to find the best solution.

References

Castany G. 1982. *Principes et méthodes de l'hydrogéologie*. Bordas, Paris.

Chang D., Vinegar H., Morriss C., and Straley C. 1997. Effective porosity, producible fluid and permeability from NMR logging. *The Log Analyst*, March-April, 60-72.

Dunn K.-J., Bergman D.J., and Latorraca G.A. 2002. *Nuclear magnetic resonance petrophysical and logging applications*. Elsevier Science Ltd, UK.

Farrar T.C., and Becker E.D. 1971. *Pulse and Fourier transform NMR*. Academic Press, Inc, New York.

Kenyon W.E., Day P.I., Starley C., and Willemsen J.F. 1988. A three-part study of NMR longtitudal relaxation properties of water-saturated sandstones. *SPE Formation Evaluation*, September 1988, 622-636.

Kenyon W.E. 1997. Petrophysical Principles of Applications of NMR Logging. *The Log Analyst*, March-April, 21-43.

Kleinberg R.L., Kenyon W.E., and Mitra P.P. 1994. Mechanism of NMR relaxation of fluids in rock. *Journal of Magnetic Resonance*, Series A 108, 206-214.

Legchenko A., and Valla P. 1998. Processing of surface proton magnetic resonance signals using non-linear fitting. *Journal of Applied Geophysics* 39, 77-83.

Legchenko A.V., Beauce A., Guillen A., Valla P., and Bernard J. 1997. Natural variations in the magnetic resonance signal used in PMR groundwater prospecting from the surface. *European Journal of Environmental and Engineering Geophysics*, 2, 173-190.

Legchenko A.V., and Shushakov O.A. 1998. Inversion of surface NMR data. *Geophysics*, 63 (1), 75-84.

Legchenko A., and Valla P. 2002a. A review of the basic principles for proton magnetic resonance sounding measurements. *Journal of Applied Geophysics*, 50, 3-19.

Legchenko A., Baltassat J-M., Beauce A., and Bernard J. 2002b. Nuclear magnetic resonance as a geophysical tool for hydrogeologists. *Journal of Applied Geophysics*, 50, 21-46.

Legchenko A., Baltassat J-M., and Vouillamoz J-M. 2003. A complex geophysical approach to the problem of groundwater investigation. In proceedings of the *Symposium on Application of Geophysics to Engineering and Environmental Problems (SAGEEP) Annual Meeting*, 6-10 April 2003, San Antonio, USA.

Schirov M., Legchenko A., and Creer G. 1991. New direct non-invasive ground water detection technology for Australia. *Exploration Geophysics*, 22, 333-338.

Seevers D.O. 1966. A nuclear magnetic method for determining the permeability of sandstones. *Paper L, in Annual Logging Symposium Transactions: Society of Professional Well Log Analysts.*

Semenov A.G., Schirov M.D., Legchenko A.V., Burshtein, and A.I., Pusep A.,Yu. 1989. Device for measuring the parameter of underground mineral deposit. *G.B. Patent* 2198540B.

Slichter C.P. 1990. In *Principles of magnetic resonance*. 3rd edition, Springer-Ferlag, Berlin Heidelberg.

Tikhonov A., and Arsenin V. 1977. In *Solution of ill-posed problems*. John Wiley & Sons, Inc.

Timur A. 1968. An Investigation of permeability, porocity, and residual water saturation relationship. *Paper K, in Annual Logging Symposium Transactions: Society of Professional Well Log Analysts.*

Timur A. 1969a. Producible porocity and permeability of sandstones investigated through nuclear magnetic resonance principles. *The Log Analist*, January-February, 3-11.

Timur A., 1969b. Pulsed nuclear magnetic resonance studies of porosity, moveable fluid, and permeability of sandstones. *Journal of Petroleum Technology*, 21, 775-786.

Trushkin D.V., Shushakov O.A., and Legchenko A.V. 1994. The potential of a noise-reducing antenna for surface NMR ground water surveys in the earth's magnetic field. *Geophysical Prospecting*, 42, 855-862.

Weichman P.B., Lavely E.M., Ritzwoller M.H. 2000. Theory of surface nuclear magnetic resonance with applications to geophysical imaging problems. *Physcal Review*, E 62, 1290-1312.

Wyllie M.R.J., and Spangler M.B. 1952. Application of electrical resistivity measurements to problem of fluid flow in porous media. *AAPG Bulletin*, 36, N2, 359-403.

ANNEXE I : MRS field results

Site: Denmark, Saby, Site_2
Loop: 2 - 75.0 Date: 27.08.2003 Time: 11:21

NUMIS data set: C:\moi\REPORTS\Denmark_2003\RMP\data_inversion\saby\SABY_2.inp
matrix: C:\moi\REPORTS\Denmark_2003\RMP\matrix\DAN_75.MRM
loop: square, side = 75.0 m
geomagnetic field:
inclination= 70 degr, magnitude= 50171.36 nT

filtering window = 159.1 ms
time constant = 15.00 ms
average S/N = 0.99; EN/IN = 13.66
fitting error: FID1 = 21.54%; FID2 = 55.15 %
param. of regular.: E,T2* = 10000.0; T1* = 70.000
permeability constant Cp = 7.00e-09

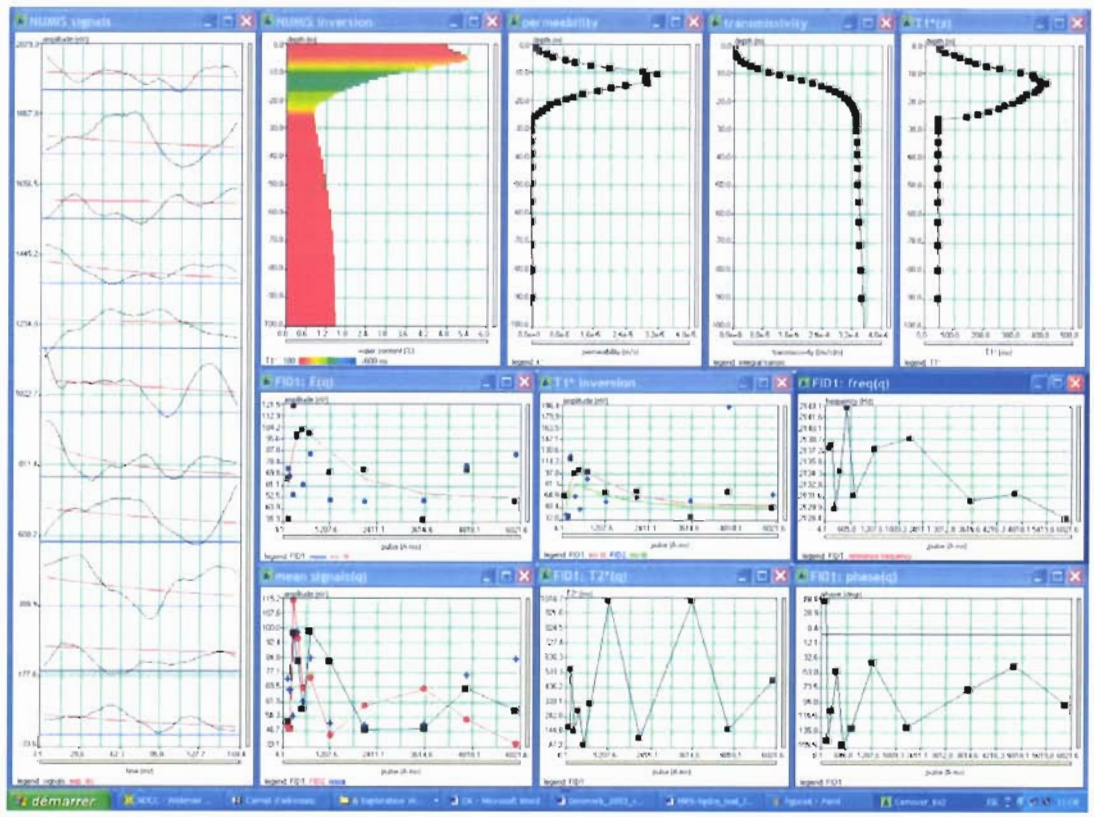

Site: Denmark, Nosby, Site_1
Loop: 2 - 75.0 Date: 28.08.2003 Time: 12:55

NUMIS data set: C:\moi\REPORTS\Denmark_2003\RMP\data_inversion\Nosby\NOSB_1.inp
matrix: C:\moi\REPORTS\Denmark_2003\RMP\matrix\DAN_75.MRM
loop: square, side = 75.0 m
geomagnetic field:
inclination= 70 degr, magnitude= 50042.25 nT

filtering window = 198.9 ms
time constant = 15.00 ms
average S/N = 0.80; EN/IN = 26.79
fitting error: FID1 = 15.55%; FID2 = 42.08 %
param. of regular.: E,T2* = 284.2; T1* = 10.000
permeability constant Cp = 7.00e-09

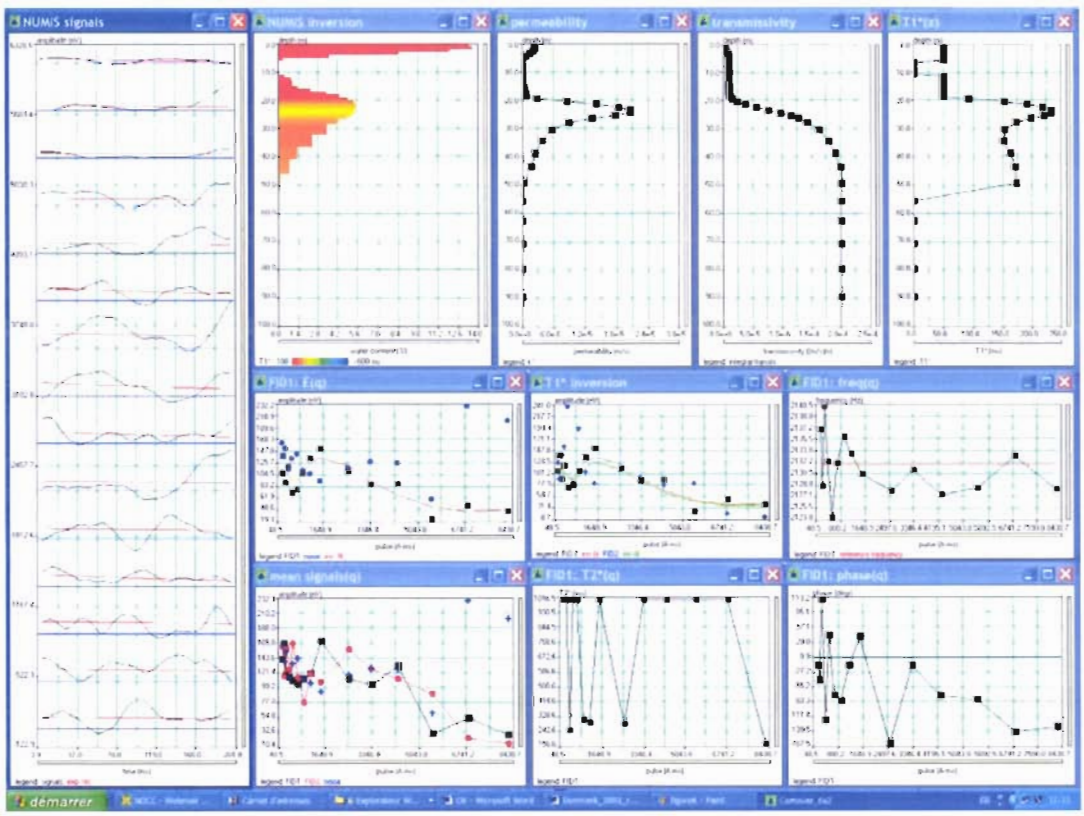

Site: Denmark, Hogsted, Site_1
Loop: 2 - 75.0 Date: 23.08.2003 Time: 11:13

NUMIS data set:
C:\moi\REPORTS\Denmark_2003\interpretation\data_inversion\Hogsted\HOGST_1B.inp
matrix: C:\moi\REPORTS\Denmark_2003\interpretation\matrix\DAN_75.MRM
loop: square, side = 75.0 m
geomagnetic field:
inclination= 70 degr, magnitude= 50171.36 nT

filtering window = 198.4 ms
time constant = 15.00 ms
average S/N = 1.58; EN/IN = 15.50
fitting error: FID1 = 19.16%; FID2 = 36.55 %
param. of regular.: E,T2* = 8000.0; T1* = 90.000
permeability constant Cp = 7.00e-09

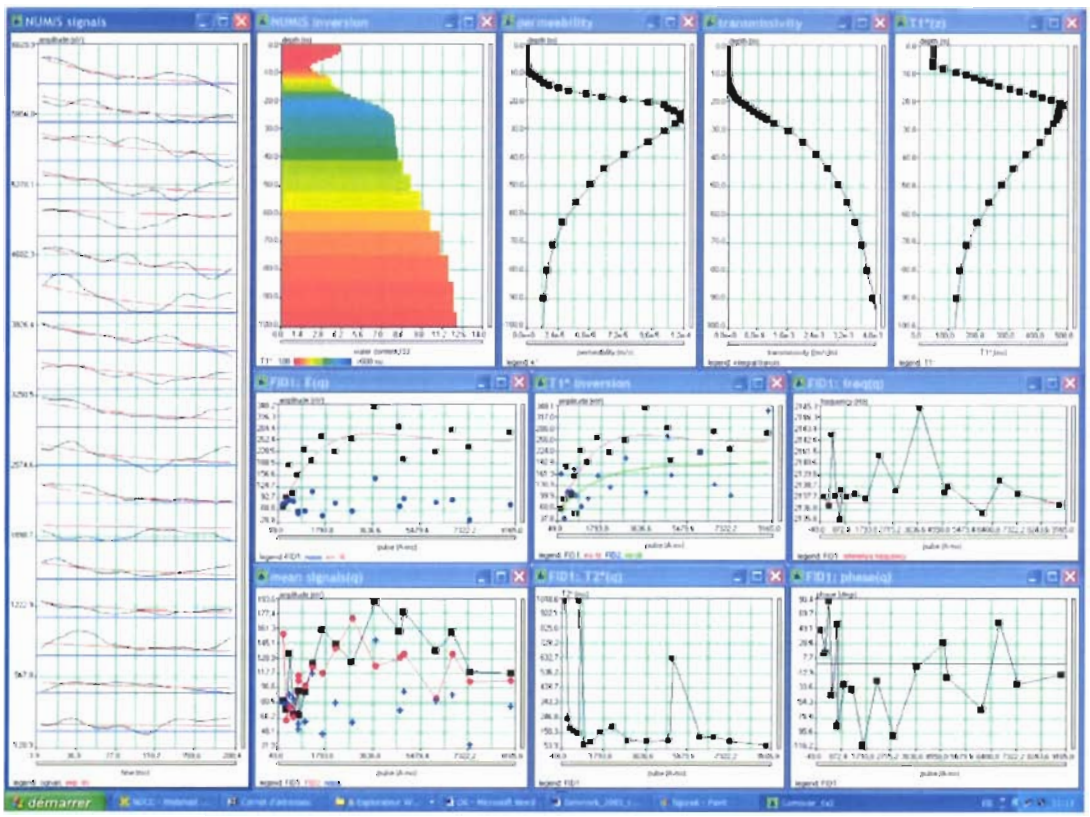

Site: Denmark, Hogsted, Site_2
Loop: 2 - 75.0 Date: 24.08.2003 Time: 10:08

NUMIS data set: C:\moi\REPORTS\Denmark_2003\interpretation\data_inversion\HOGST_2.inp
matrix: C:\moi\REPORTS\Denmark_2003\interpretation\matrix\DAN_75.MRM
loop: square, side = 75.0 m
geomagnetic field:
inclination= 70 degr, magnitude= 50201.88 nT

filtering window = 198.3 ms
time constant = 35.00 ms
average S/N = 1.57; EN/IN = 11.88
fitting error: FID1 = 27.54%; FID2 = 23.66 %
param. of regular.: E,T2* = 5000.0; T1* = 70.000
permeability constant Cp = 7.00e-09

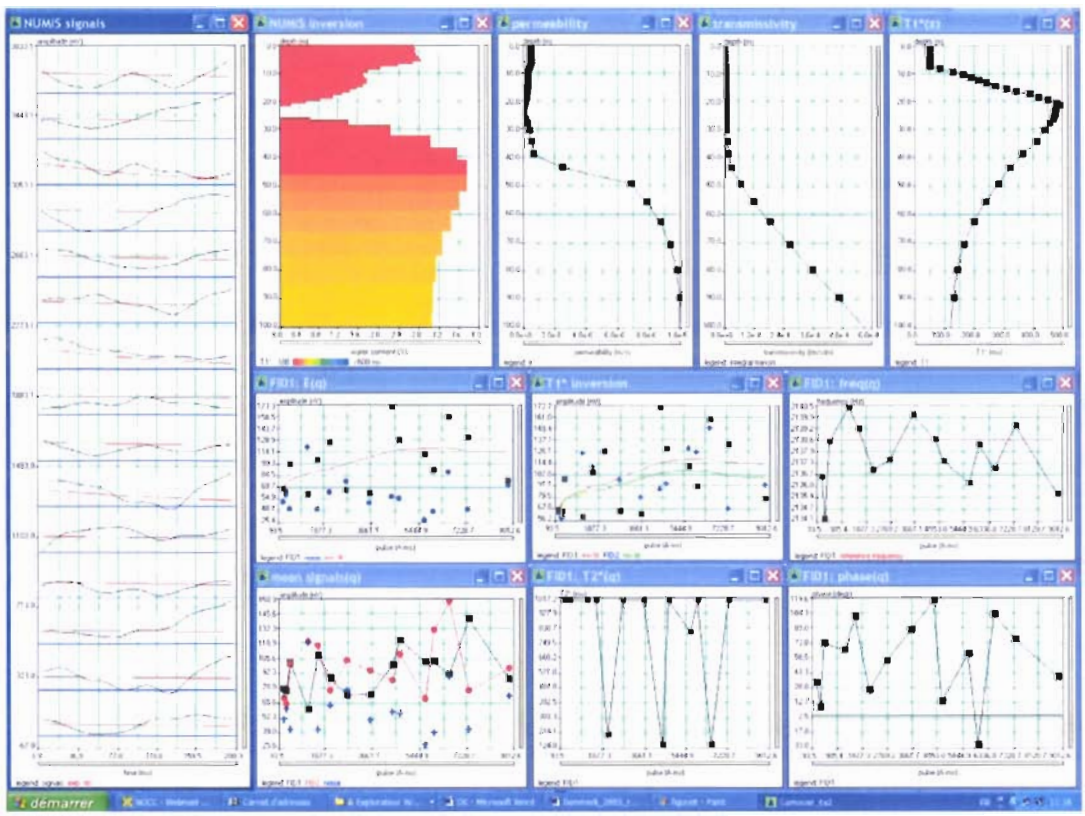

Site: Denmark, Hogsted, Site_3
Loop: 2 - 75.0 Date: 25.08.2003 Time: 15:28

NUMIS data set: C:\moi\REPORTS\Denmark_2003\interpretation\data_inversion\HOGST_3.inp
matrix: C:\moi\REPORTS\Denmark_2003\interpretation\matrix\DAN_75.MRM
loop: square, side = 75.0 m
geomagnetic field:
inclination= 70 degr, magnitude= 50171.36 nT

filtering window = 198.4 ms
time constant = 15.00 ms
average S/N = 2.07; EN/IN = 7.08
fitting error: FID1 = 20.77%; FID2 = 30.31 %
param. of regular.: modeling
permeability constant Cp = 7.00e-09

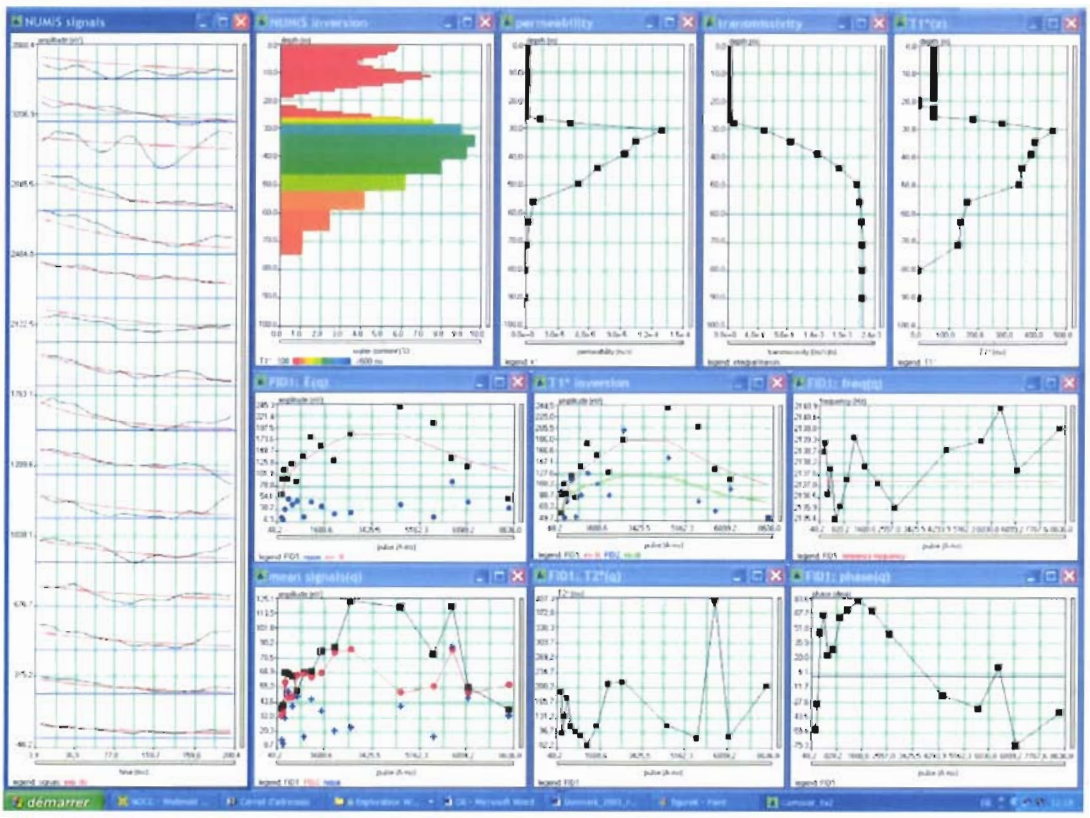

Site: Denmark, Hogsted, Site_4
Loop: 2 - 75.0 Date: 26.08.2003 Time: 19:04

NUMIS data set: C:\moi\REPORTS\Denmark_2003\RMP\data_inversion\Hogsted\HOGST_4.inp
matrix: C:\moi\REPORTS\Denmark_2003\RMP\matrix\DAN_75.MRM
loop: square, side = 75.0 m
geomagnetic field:
inclination= 70 degr, magnitude= 50171.36 nT

filtering window = 198.4 ms
bandpass = 5.00 Hz
average S/N = 1.24; EN/IN = 29.37
fitting error: FID1 = 23.02%; FID2 = 34.15 %
param. of regular.: E,T2* = 8000.0; T1* = 90.000
permeability constant Cp = 7.00e-09

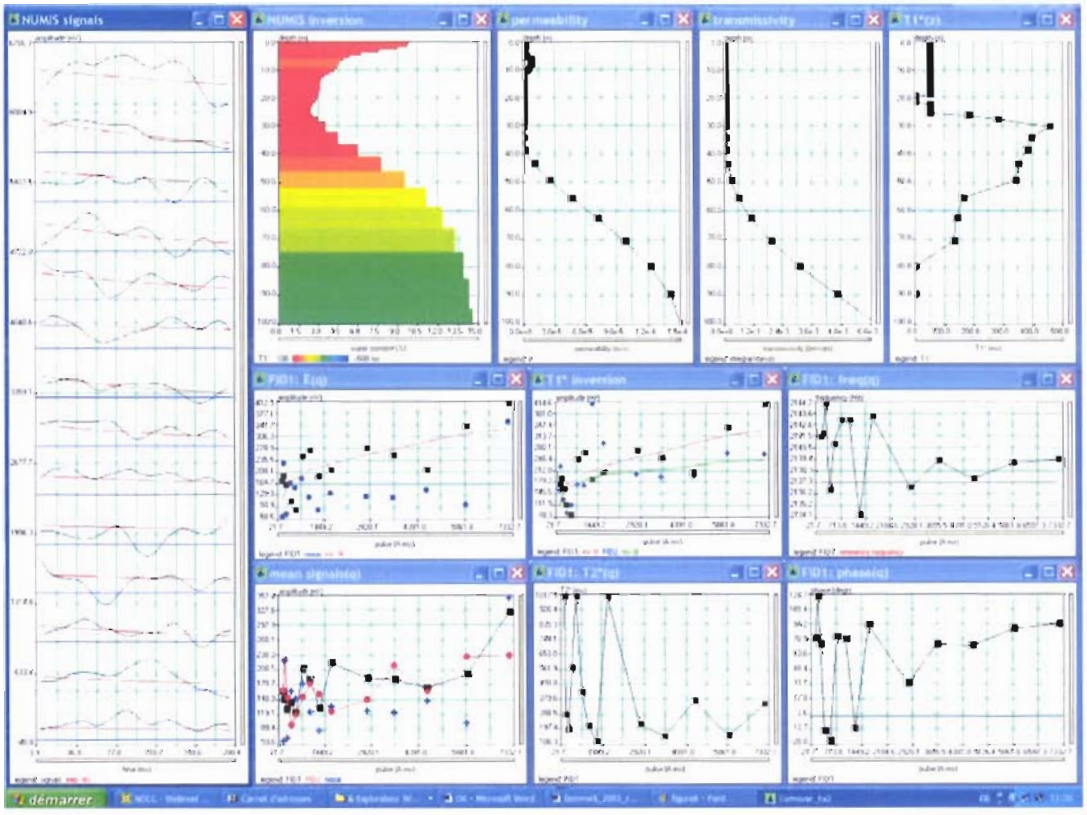

Site: Denmark, Hogsted, Site_5
Loop: 2 - 75.0 Date: 28.08.2003 Time: 20:09

NUMIS data set: C:\moi\REPORTS\Denmark_2003\RMP\data_inversion\Hogsted\HOGST_5.inp
matrix: C:\moi\REPORTS\Denmark_2003\RMP\matrix\DAN_75.MRM
loop: square, side = 75.0 m
geomagnetic field:
inclination= 70 degr, magnitude= 50171.36 nT

filtering window = 198.4 ms
time constant = 15.00 ms
average S/N = 3.01; EN/IN = 6.89
fitting error: FID1 = 10.44%; FID2 = 27.94 %
param. of regular.: E,T2* = 1500.0; T1* = 30.000
permeability constant Cp = 7.00e-09